Report

Comparative analyses of aging-related genes in long-lived mammals provide insights into natural longevity

Zhenpeng Yu,[1] Inge Seim,[1,2,3] Mengxin Yin,[1] Ran Tian,[1] Di Sun,[1] Wenhua Ren,[1] Guang Yang,[1,*] and Shixia Xu[1,*]
*Correspondence: gyang@njnu.edu.cn (G.Y.); xushixia78@163.com (S.X.)
Received: October 11, 2020; Accepted: April 26, 2021; Published Online: April 28, 2021; https://doi.org/10.1016/j.xinn.2021.100108

Graphical abstract

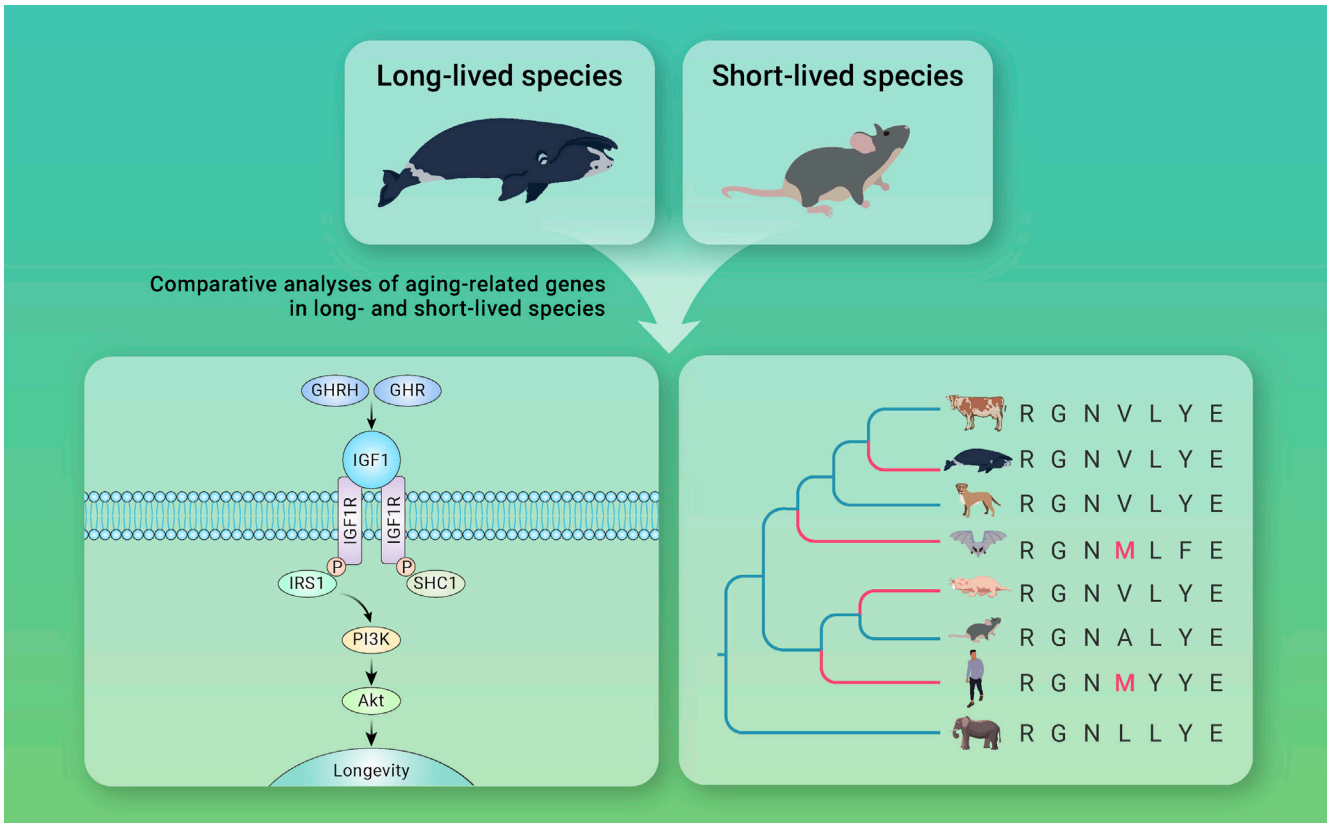

Public summary

- Evolution analyses of 115 aging-related genes exploring natural longevity in mammals
- Positively selected genes & rapidly evolved genes enriched in IIS and immune pathways
- Convergent mutations in genes associated with cancer in long-lived species
- Evolution of longevity through cancer resistance in long-lived mammals

Report

Comparative analyses of aging-related genes in long-lived mammals provide insights into natural longevity

Zhenpeng Yu,[1] Inge Seim,[1,2,3] Mengxin Yin,[1] Ran Tian,[1] Di Sun,[1] Wenhua Ren,[1] Guang Yang,[1,*] and Shixia Xu[1,*]

[1]Jiangsu Key Laboratory for Biodiversity and Biotechnology, College of Life Sciences, Nanjing Normal University, Nanjing 210023, China

[2]Integrative Biology Laboratory, College of Life Sciences, Nanjing Normal University, Nanjing 210023, China

[3]School of Biology and Environmental Science, Faculty of Science and Engineering, Queensland University of Technology, Brisbane, QLD, Australia

*Correspondence: gyang@njnu.edu.cn (G.Y.); xushixia78@163.com (S.X.)

Received: October 11, 2020; Accepted: April 26, 2021; Published Online: April 28, 2021; https://doi.org/10.1016/j.xinn.2021.100108

Citation: Yu Z., Seim I., Yin M., et al., (2021). Comparative analyses of aging-related genes in long-lived mammals provide insights into natural longevity. The Innovation **2(2)**, 100108.

Extreme longevity has evolved multiple times during the evolution of mammals, yet its underlying molecular mechanisms remain largely underexplored. Here, we compared the evolution of 115 aging-related genes in 11 long-lived species and 25 mammals with non-increased lifespan (control group) in the hopes of better understanding the common molecular mechanisms behind longevity. We identified 16 unique positively selected genes and 23 rapidly evolving genes in long-lived species, which included nine genes involved in regulating lifespan through the insulin/IGF-1 signaling (IIS) pathway and 11 genes highly enriched in immune-response-related pathways, suggesting that the IIS pathway and immune response play a particularly important role in exceptional mammalian longevity. Interestingly, 11 genes related to cancer progression, including four positively selected genes and seven genes with convergent amino acid changes, were shared by two or more long-lived lineages, indicating that long-lived mammals might have evolved convergent or similar mechanisms of cancer resistance that extended their lifespan. This suggestion was further corroborated by our identification of 12 robust candidates for longevity-related genes closely related to cancer.

Keywords: mammals; longevity; positive selection; IIS pathway; immune response; cancer resistance

INTRODUCTION

Extant mammals differ dramatically in their maximum lifespans, ranging from a little over 1 year (e.g., forest shrews, *Myosorex varius*) to more than 200 years (e.g., bowhead whales, *Balaena mysticetus*), a difference of more than 100-fold.[1] In general, larger species tend to live longer than smaller ones, presumably due to higher intrinsic fitness (i.e., stress resistance) and a lack of apex predators.[2] For example, the bowhead whale has an estimated maximum lifespan of 211 years and a body mass of more than 100 tons.[3,4] The African elephant (*Loxodonta africana*), the largest land mammal, weighs more than 6 tons and lives up to 65 years.[5] However, some species defy this apparent correlation between large body size and longevity. Brandt's bat (*Myotis brandtii*) weighs 5–20 g and lives for more than 40 years,[6] while the naked mole rat (*Heterocephalus glaber*) lives for more than 30 years—ten times longer than other similar-sized rodents.[7,8] Similar to large long-lived mammals, Brandt's bat and the naked mole rat reduce predation risk through flight/cave-dwelling and a subterranean lifestyle, respectively.[9] To allow for cross-species comparisons of longevity, Austad and Fisher introduced the longevity quotient, maximum lifespan corrected for body size.[10] Employing this variable, the longevity of many bats and subterranean rodents is striking. Thus, species such as the bowhead whale, African elephant, Brandt's bat, and naked mole rat are well positioned to evolve a longer lifespan.

To achieve longevity, species must evolve better mechanisms to attenuate aging (organismal senescence) and related diseases (e.g., cancer). The current consensus is that aging in diverse species is manifested by distinct hallmarks and that the aging process (and lifespan) can be modulated in various ways—by environmental, genetic, or pharmacological interventions.[11] Over the past few decades, numerous aging-related genes have been identified from experiments on model animals (e.g., mouse, fruit fly, and worm).[11] However, we do not know whether some of these genes are involved in controlling lifespan variations during the evolution of species. In recent years, aging research has paid more attention to long-lived mammals.[12–16] For example, the small-sized naked mole rat experienced unique coding changes in its *HAS2* (Hyaluronan Synthase 2) gene and secretes high-molecular-mass hyaluronan, a polysaccharide that likely mediates early contact inhibition and contributes to cancer resistance.[16] A comparative study of liver transcriptomics among mice, naked mole rats, and humans revealed that DNA-repair genes of long-lived species are upregulated compared with those of short-lived mice,[17] which agrees with the argument that DNA repair plays a vital role in longevity.[11] A similar result was found in long-lived whales: genes linked to DNA repair and cancer resistance were found to be under positive selection and were found to have specific mutations in the bowhead whale and humpback whale (*Megaptera novaeangliae*).[12,13] Importantly, 12–20 copies of the tumor-suppressor gene *TP53* were uniquely identified in the genome of elephants, helping to reduce their cancer incidence by increasing their cellular sensitivity to DNA damage.[14]

It is worth noting that lifespans may be extended by both specific adaptations and shared mechanisms. Better understanding of the latter requires identifying the molecular mechanisms that underlie extended lifespans across mammalian phylogeny, which in turn requires the analysis of aging-related genes shared by long-lived species. In this study, we considered the molecular evolution of aging-associated genes in GenAge, a curated database of genes generated by surveying human disease data (e.g., genes associated with a longer lifespan in a population) and genetic perturbation experiments in animal models.[1,18] Making use of 115 aging-related genes and 36 species spanning 14 mammal orders, we searched for the genes or pathways that may contribute to extending lifespan in mammals.

RESULTS

The maximum lifespan and body mass of 987 mammalian species were obtained from the AnAge database.[1] We calculated each species' longevity quotient based on the allometric equation for all mammals (see supplemental materials and methods).[19] The mean longevity quotient value ± standard deviation (SD) for all mammals was 1 ± 0.57 (Table 1). In our 36-species dataset, 11 species had a longevity quotient value of >1.57 and were classified as long-lived: human (*Homo sapiens*), Sumatran orangutan (*Pongo abelii*), pigtailed macaque (*Macaca nemestrina*), common marmoset (*Callithrix jacchus*), gray mouse lemur (*Microcebus murinus*), naked mole rat (*H. glaber*), bowhead whale (*B. mysticetus*), killer whale (*Orcinus orca*), Brandt's bat

Table 1. Mean values of MLS (maximum lifespan) and LQ (longevity quotient) computed using 987 species' records from the AnAge database

	n[a]	MLS mean	MLS SD[b]	MLS limits	LQ mean	LQ SD	LQ limits
Peramelemorphia	9	5.93	1.96	3.97–7.89	0.37	0.12	0.25–0.49
Monotremata	3	37.77	13.77	24.00–51.54	1.91	0.60	1.31–2.51
Diprotodontia	52	15.85	6.31	9.54–22.16	0.79	0.26	0.53–1.05
Dasyuromorphia	19	6.32	2.39	3.93–8.71	0.50	0.13	0.37–0.63
Primates	153	31.31	12.67	18.64–43.98	1.60	0.43	1.17–2.03
Scandentia	5	11.76	0.53	11.23–12.29	0.91	0.22	0.69–1.13
Cetartiodactyla	177	29.61	22.76	6.85–52.37	0.83	0.30	0.53–1.13
Chiroptera	88	17.62	7.77	9.85–25.39	1.77	0.86	0.91–2.63
Lagomorpha	12	10.07	3.09	6.98–13.16	0.59	0.13	0.46–0.72
Eulipotyphla	17	5.40	3.51	1.89–8.91	0.44	0.17	0.27–0.61
Rodentia	230	9.45	5.68	3.77–15.13	0.68	0.33	0.35–1.01
Afrotheria	19	24.77	24.65	0.12–49.42	0.94	0.45	0.49–1.39
Perissodactyla	15	38.16	8.49	29.67–46.65	1.00	0.23	0.77–1.23
Carnivora	159	20.87	8.66	12.21–29.53	0.94	0.27	0.67–1.21
Pilosa	5	28.76	10.93	17.83–39.69	1.31	0.50	0.81–1.81
Cingulata	8	20.86	7.74	13.12–28.60	1.10	0.47	0.63–1.57
Didelphimorphia	16	4.88	1.84	3.04–6.72	0.38	0.15	0.23–0.53
Total	987	20.15	15.58	4.60–35.80	1.00	0.57	0.43–1.57

[a]Number of species included in each order.
[b]SD, standard deviation.

(*M. brandtii*), little brown bat (*Myotis lucifugus*), and Hoffman's two-toed sloth (*Choloepus hoffmanni*) (Figure 1).

Selective pressure test of aging-related genes across mammals

Under lower adult mortality rates, selection will favor gene changes that confer a later maturity and longer lifespan.[20,21] To test for divergent evolution patterns between the long-lived and control groups, we performed clade model C, revealing that 20% (23/115) of the genes in the long-lived group were rapidly evolving genes (Table 2). Of these genes, three (*INSR*, *IRS1*, and *PIK3CB*) are associated with the process of signal transduction by insulin receptor kinase and two (*ATM* [ataxia telangiectasia mutated] and *ERCC6*) with DNA repair. Moreover, nine genes (*BCL2*, *CDC42*, *DGAT1*, *GRN*, *PIK3CB*, *PLCG2*, *STAT5A*, *STAT5B*, and *VCP*) are involved in the immune process.

The branch-site model was further used to identify positively selected genes on each branch across the phylogeny. A total of 29.57% (34/115) of the aging-related genes were identified to be under positive selection in the long-lived group after p-value adjustment (Table S3). Of them, 18 genes were also identified in the control groups; however, 16 genes were in at least one of the 11 long-lived lineages (Figure 2A and Table S4). For example, five (*CTGF*, *BCL2*, *GHRH*, *DBN1*, and *ERCC3*) and two (*CTGF* and *DBN1*) genes were under positive selection along the branches leading to the little brown bat and Brandt's bat, respectively (Table S4). In addition, four positively selected genes were determined in two long-lived species: *PDGFRB* in the little brown bat and sloth; and *CTGF*, *DBN1*, and *ABL1* in both the little brown bat and Brandt's bat (i.e., genus *Myotis*) (Table S3).

The proportion of positively selected genes identified in the long-lived species was larger than that in the control group for genes related to immunity, metabolism, growth regulation, signal transduction, transcription regulation, cancer, and apoptosis, based on the GeneCards description (Figure 2B). In addition, we evaluated the functional enrichment of positively selected genes using gene ontology (GO) and Kyoto Encyclopedia of Genes and Genomes (KEGG) annotations. The 16 long-lived group-specific positively selected genes were significantly enriched for immune progress, such as lymphocyte proliferation, response to interleukin, and interleukin-2-mediated signaling pathway (Figure 2C). These genes were also over-represented in several KEGG pathways, including endocrine resistance (i.e., estrogen resistance in breast cancer), focal adhesion, and the AGE-RAGE signaling pathway in diabetic complications (Figure 2D). In contrast, the genes under positive selection in the control group were enriched for DNA repair, the cell cycle, ERK1 and ERK2 signaling, and nucleotide excision repair (Figures 2B–2D and Table S5). In addition, 18 positively selected genes shared by two groups were enriched for the regulation of mitogen-activated protein (MAP) kinase activity and the phosphatidylinositol 3-kinase (PI3K)-Akt signaling pathway (Figures 2C and 2D).

Convergent amino acid substitutions between long-lived species

To assess convergent evolution in long-lived species, we first reconstructed ancestral sequences for the internal nodes of the species tree to identify shared amino acid substitutions along lineages leading to extreme longevity based on the JTT-f_{genes} model. We then found three convergent amino acid changes in the distant species, including one change (*BLM*: S579P) in the naked mole rat and killer whale, and two substitutions (*ERBB2*: P385Q and *GRN*: S371N) in the lineages leading to the bowhead and killer whales (Figure 1). Furthermore, five long-lived group-specific unique amino acid changes were also determined in four genes: *EGFR* (V111M), *PEX5* (R396Q), *PLCG2* (L517V, V967I), and *PRKCD* (K621R) (Figure 1). For example, the long-lived primates and bats (genus *Myotis*) had three convergent substitutions in *EGFR*, *PEX5*, and *PLCG2* (Figure 1).

Gene-phenotype coevolution

To assess the relationship between the rate of gene evolution and aging-associated life-history traits, we performed a univariate linear regression

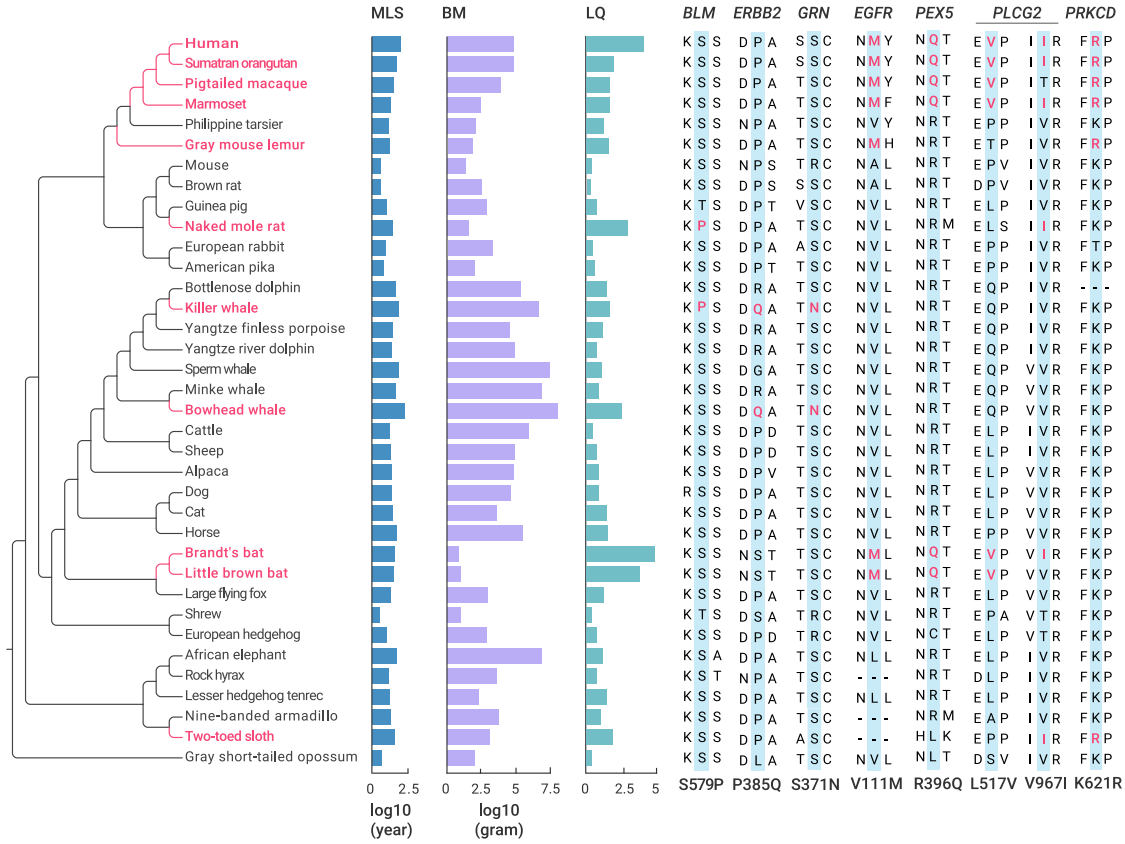

Figure 1. The phylogeny of the mammals used for this study alongside their life-history traits Long-lived mammals are marked on red on the left-hand side of the figure. Life-history traits, including maximum lifespan (MLS), body mass (BM), and longevity quotient (LQ), are displayed in the middle. Seven cancer-associated genes showed convergent amino acid substitutions within long-lived mammals, which are listed in the right-hand side of the figure (long-lived species-specific amino acid changes are colored red).

analysis of maximum lifespan and two other longevity-associated traits (body mass and longevity quotient) obtained from AnAge. As expected,[22] the analyses revealed a significant association: maximum lifespan covaries with body mass (R^2 = 0.47, $p < 2.17 \times 10^{-6}$) and longevity quotient (R^2 = 0.57, $p < 5.19 \times 10^{-8}$). Multiple linear regression followed by a type I analysis of variance revealed that longevity quotient was the best predictor, accounting for 50% of the maximum lifespan variance ($p < 2 \times 10^{-16}$), whereas body mass accounted for 47% of the remaining variance and the remainder (3%) was residual error (Figure S1).

Pagel's λ model, used to assess the phylogenetic signal, showed that phylogeny explained a high proportion of the variance in mammalian maximum lifespan (λ = 0.97), body mass (λ = 0.99), and longevity quotient (λ = 0.97) (Table S6). We next employed the phylogenetic generalized least-squares method to assess correlations between the evolutionary rate of genes (root-to-tip d_N/d_S) and longevity-associated traits. Phylogenetic generalized least-squares analysis revealed that the evolutionary rates of nine genes (*ARNTL*, *ATM*, *BMI1*, *CDK1*, *CTNNB1*, *ERCC3*, *ERCC5*, *NRG1*, and *STAT5A*) are associated with maximum lifespan (Table S7). Seven genes (*BMI1*, *CTNNB1*, *E2F1*, *ERBB2*, *IGF1*, *IGF1R*, and *PDGFB*) exhibited an association with body mass, while four (*CDK1*, *ERCC3*, *HRAS*, and *INSR*) showed an association with longevity quotient (Table S7). These 16 genes associated with one or more longevity-associated phenotypes were regarded as longevity-associated genes. Notably, the evolutionary rates of both *CDK1* and *ERCC3* showed an association with both maximum lifespan and longevity quotient, while the rate of *BMI1* was associated with maximum lifespan and body mass (Figure 3). Interestingly, a negative correlation was found between body mass and the evolutionary rates of two genes, *IGF1R* and *IGF1* (Table S7). Specifically, these 16 longevity-associated genes were particularly enriched in several KEGG pathways, including prostate cancer, breast cancer, and the Rap1 signaling pathway. In addition, the 16 longevity-associated genes were also significantly assigned to GO terms such as regulation of cell-cycle processes and cell aging, disease ontology (DO) terms including female reproductive organ cancer, sarcoma, and hereditary breast ovarian cancer, and Reactome pathways, including signaling by receptor tyrosine kinases and diseases of signal transduction (Figure 4).

Overlap among different datasets

Our results revealed 23 rapidly evolving genes, 16 positively selected genes, and 16 longevity-associated genes in the long-lived group. There was some overlap among the three types of genes: five genes (*BCL2*, *EGR1*, *NCOR1*, *STAT5B*, and *VCP*) were identified as both positively selected and rapidly evolving genes, four (*ARNTL*, *ATM*, *INSR*, and *STAT5A*) were both rapidly evolving and longevity-associated genes, and three (*ERBB2*, *ERCC3*, and *IGF1*) were both positively selected and longevity-associated genes (Figure 5A). Importantly, these overlapping genes were involved in DNA repair (*ERCC3* and *ATM*), immune processes (*BCL2*, *STAT5A*, *STAT5B*, and *VCP*), and the insulin/IGF-1 signaling (IIS) pathway (*IGF1* and *INSR*), which are essential for inhibiting tumorigenesis or longevity. Therefore, these 12 genes can be considered robust candidates of longevity-related genes. We further used the protein-protein interactions database STRING (http://www.string-db.org) to explore the interactions among the rapidly evolving genes, positively selected genes, and longevity-associated genes, and found that all these genes interacted with each other ($p < 1.0 \times 10^{-16}$, Figure 5B). Specifically, the top genes with relatively high degrees of connectivity (≥10 degrees) were involved in the IIS pathway: *GHR* (11), *IRS1* (10), *PTPN1* (11), and *SHC1* (13). In addition, three genes related to DNA repair interacted with each other: *ERCC3* (2), *ERCC5* (2), and *ERCC6* (3).

Table 2. List of rapidly evolving genes in long-lived group identified using the clade model C

				Parameter estimates				
Gene	**-lnLCmC**	**-lnLM2a_rel**	**p value**	**Proportion**	**ω_0**	**ω_1**	**Background ω**	**Foreground ω**
ARNTL	7,351.482	7,355.586	0.004	p_0 = 0.892; p_1 = 0.005; p_2 = 0.102	0.005	1.000	0.107	0.432
ATM	51,496.600	51,509.852	0.000	p_0 = 0.595; p_1 = 0.063; p_2 = 0.343	0.025	1.000	0.300	0.491
BCL2	2,542.311	2,545.377	0.013	p_0 = 0.859; p_1 = 0.000; p_2 = 0.141	0.014	1.000	0.160	0.714
CDC42	2,300.064	2,303.047	0.015	p_0 = 0.066; p_1 = 0.000; p_2 = 0.934	0.094	1.000	0.000	0.039
DGAT1	8,002.016	8,007.764	0.001	p_0 = 0.765; p_1 = 0.019; p_2 = 0.216	0.008	1.000	0.164	0.413
EFEMP1	8,311.676	8,315.715	0.004	p_0 = 0.758; p_1 = 0.025; p_2 = 0.217	0.010	1.000	0.185	0.412
EGR1	9,962.475	9,964.822	0.030	p_0 = 0.717; p_1 = 0.003; p_2 = 0.280	0.005	1.000	0.127	0.205
ERCC6	16,782.841	16,785.213	0.029	p_0 = 0.739; p_1 = 0.033; p_2 = 0.228	0.014	1.000	0.234	0.365
FGF23	2,670.472	2,673.045	0.023	p_0 = 0.690; p_1 = 0.023; p_2 = 0.287	0.022	1.000	0.194	0.463
GHR	9,743.770	9,746.715	0.015	p_0 = 0.583; p_1 = 0.041; p_2 = 0.376	0.029	1.000	0.328	0.542
GRN	12,342.258	12,346.864	0.002	p_0 = 0.530; p_1 = 0.136; p_2 = 0.334	0.006	1.000	0.211	0.354
HBP1	7,950.469	7,953.984	0.008	p_0 = 0.726; p_1 = 0.026; p_2 = 0.249	0.003	1.000	0.189	0.417
HESX1	2,960.034	2,965.417	0.001	p_0 = 0.541; p_1 = 0.112; p_2 = 0.347	0.011	1.000	0.210	0.771
INSR	27,632.398	27,638.724	0.000	p_0 = 0.811; p_1 = 0.004; p_2 = 0.185	0.006	1.000	0.121	0.197
IRS1	19,448.998	19,451.540	0.024	p_0 = 0.834; p_1 = 0.015; p_2 = 0.151	0.007	1.000	0.157	0.244
NCOR1	31,049.485	31,051.550	0.042	p_0 = 0.784; p_1 = 0.017; p_2 = 0.198	0.014	1.000	0.252	0.326
PDGFRB	22,001.509	22,005.606	0.004	p_0 = 0.732; p_1 = 0.028; p_2 = 0.240	0.010	1.000	0.199	0.296
PIK3CB	14,288.132	14,292.053	0.005	p_0 = 0.777; p_1 = 0.008; p_2 = 0.214	0.007	1.000	0.185	0.345
PLCG2	24,791.961	24,795.709	0.006	p_0 = 0.810; p_1 = 0.012; p_2 = 0.177	0.009	1.000	0.142	0.214
PTPN1	5,729.684	5,731.999	0.031	p_0 = 0.855; p_1 = 0.010; p_2 = 0.135	0.006	1.000	0.150	0.307
STAT5A	14,464.372	14,468.614	0.004	p_0 = 0.836; p_1 = 0.004; p_2 = 0.160	0.005	1.000	0.113	0.194
STAT5B	11,082.355	11,121.641	0.000	p_0 = 0.079; p_1 = 0.000; p_2 = 0.920	0.174	1.000	0.005	0.051
VCP	12,614.071	12,634.515	0.000	p_0 = 0.977; p_1 = 0.000; p_2 = 0.023	0.001	1.000	0.000	1.384

DISCUSSION

Long lifespan evolved multiple times during the evolution of mammals. The last decade has seen an explosion in the number of genome assemblies and amount of genomic data from several long-lived mammals, and these have revealed shared and lineage-specific changes that facilitate a long lifespan by enhancing homeostasis throughout life. Sometimes this involves the changes directly resisting tumor development or progression, as is the case for the duplication of the tumor-suppressor gene *TP53* in elephants (12–20 copies) and *FBXO31* (Forkhead box protein 31) in Brandt's bat (57 copies).[14,15] In this study, we examined the evolution of a set of 115 genes, designated "aging-associated" genes in the GenAge database,[1,18] spanning 36 mammals in 14 orders.

The IIS pathway and immune genes contribute to extending longevity

Our results identified 16 positively selected genes and 23 rapidly evolving genes in the long-lived species, which included nine genes (growth hormone receptor [*GHR*], *GHRH*, *IGF1*, *IRS1*, *INSR*, *SHC1*, *PIK3CB*, *PTPN1*, and *FOXO4* [Forkhead box protein 4]) involved in the IIS pathway, a key lifespan regulatory pathway.[23] Multiple genetic manipulations that attenuate signaling intensity at different levels of the IIS pathway extend the lifespan of mice.[24–26] For example, previous studies showed that lower IGF1 levels and GHRH knockout in mice can extend their lifespan.[26] Mice with an adipose-specific knockout of INSR live 18% longer than those without the knockout.[25] In addition, mice heterozygous for IGF1R knockout live 26% longer than wild-type mice.[27] Interestingly, consistent with our findings, a number of genes in the IIS pathway were found to have unique sequence and expression changes in long-lived species. For example, unique amino acid deletion or replacement in the GHR was identified in the small-body-size and long-lived bat species.[15] Interestingly, previous studies have revealed that mutations or deficiencies of the GHR result in human Laron-type dwarfism and increased resistance to cancer in humans and mice.[28–30] In addition, the expression of insulin receptor (INSR) protein, which regulates energy metabolism by activating the insulin signaling pathway, was recently reported to be positively correlated with longevity across mammals.[31] Taken together, genes involved in the IIS pathway were identified to be under accelerated evolution or positive selection in the long-lived lineages, which may be contributing to extending lifespan in mammals.

Our results also revealed that five positively selected genes (*BCL2*, *VCP*, *SHC1*, *EGR1*, and *STAT5B*) and nine rapidly evolving genes (*BCL2*, *CDC42*, *DGAT1*, *GRN*, *PIK3CB*, *PLCG2*, *STAT5A*, *STAT5B*, and *VCP*) identified in the long-lived species were highly enriched in immune-associated pathways, including lymphocyte proliferation, leukocyte proliferation, and the interleukin-2-mediated signaling pathway. For instance, in peripheral immune cells, PLCG2 has been implicated in the signaling pathways downstream of the B cell receptor and is thought to modulate the functions of macrophages, neutrophils, and natural killer cells through the Fc receptor.[32] As is well known, the immune system is often under strong selective pressure and has important implications for aging and disease resistance.[33] Similarly,

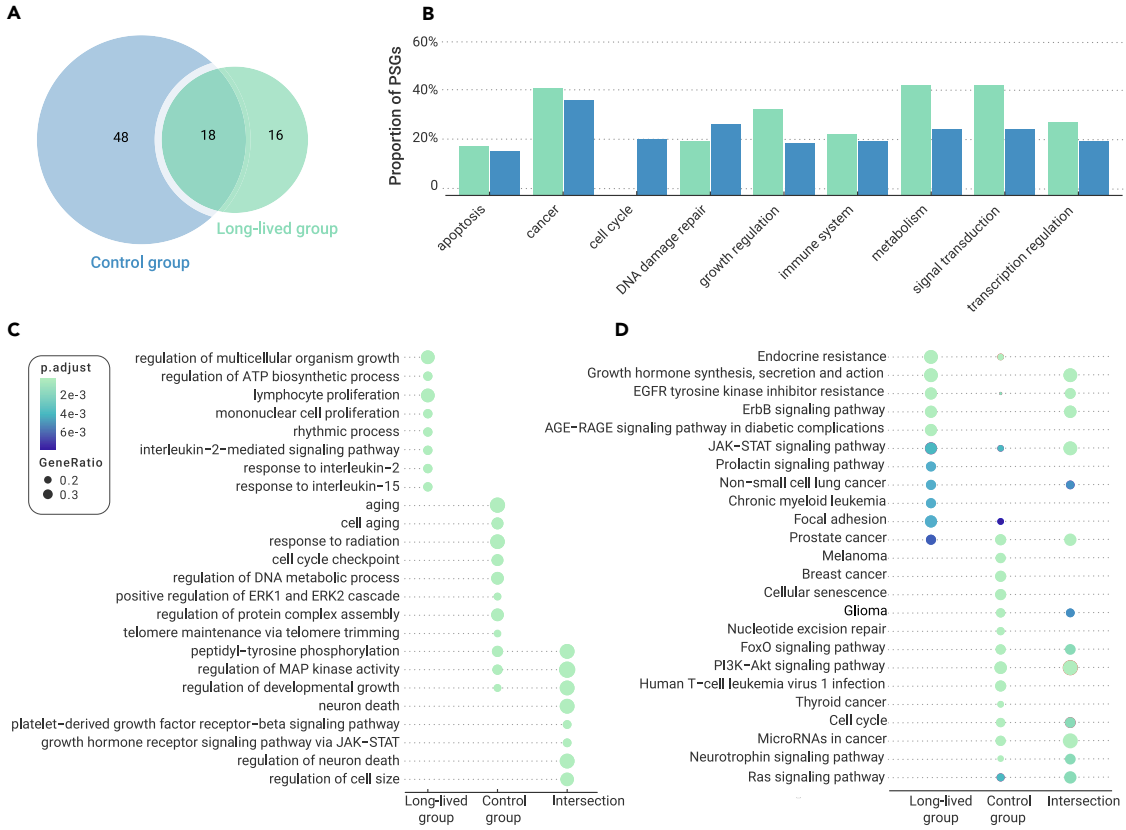

Figure 2. Functional enrichment of positively selected genes in long-lived and control species (A) Number of positively selected genes (PSGs) identified in the long-lived and control groups. (B) Proportion of positively selected genes (PSGs) for gene function in the long-lived and control groups. (C and D) GO and KEGG pathway enrichment of PSGs in long-lived and control groups. Top functional terms of biological process or pathways are shown. Circle sizes are proportional to the number of genes assigned to a pathway, and the color of the circle indicates the adjusted p value for each pathway.

previous studies identified immune-response genes to be under positive selection, expanded, and upregulated in long-lived bats, blind mole rats, and naked mole rats.[34] Importantly, the expression of immune-response genes in the liver across 33 mammalian species was positively related to maximum lifespan.[35]

In addition, comparative genomic analysis of the short-lived African turquoise killifish and exceptionally long-lived mammals revealed that some aging and longevity candidates—such as *CREBBP*, *CGNL1*, and *IGF1R*—were under positive selection in both short- and long-lived species, suggesting that the same gene could underlie the evolution of both exceptionally extended and shortened lifespans.[36] Similarly, 18 aging-related genes were detected to be under positive selection in both long-lived and control groups. These genes were significantly enriched in the PI3K-Akt signaling pathway, which is critical to the cell-cycle process and is associated with cellular quiescence, proliferation, cancer, and longevity.[37]

Genes related to cancer progression exhibit molecular convergence in long-lived species

Convergent phenotypic evolution provides unique opportunities for studying how genomes encode phenotypes. Convergence was observed at different molecular levels, such as amino acid substitutions, the same positively selected genes, and convergent shifts in amino acid preference.[38] The present study revealed that four positively selected genes (*CTGF*, *DBN1*, *ABL1*, and *PDGFRB*) related to longevity were uniquely shared by long-lived lineages. Three of these (*CTGF*, *DBN1*, and *ABL1*) were examined in the long-lived little brown bat and Brandt's bat (genus *Myotis*). *ABL1* (ABL proto-oncogene 1 non-receptor tyrosine kinase) is an oncogene that encodes a protein tyrosine kinase involved in various cellular processes, including cell division and DNA repair.[39] *PDGFRB* (platelet-derived growth factor receptor β) was determined to be under positive selection in the little brown bat and Hoffman's two-toed sloth. Previous studies showed that *PDGFRB* stimulates cell proliferation and tumor migration through an array of signaling pathways, such as MAP kinases, PI3K, and STAT (signal transducers and activators of transcription).[40]

In addition, three convergent amino acid substitutions in three genes (*GRN*, *ERBB2*, and *BLM*) were identified in the long-lived group. These genes are associated with cancer incidence and DNA repair. For example, *GRN* (granulin, a growth factor)-knockout mice exhibited decreased survival—with less than 50% of animals living more than 2 years—and signs of cellular aging.[41] *ERBB2*, commonly referred to as *HER2*, was overexpressed in 20%–30% of invasive breast carcinomas.

Moreover, five specific amino acid changes in four genes (*EGFR*, *PEX5*, *PLCG2*, and *PRKCD*) were observed in long-lived species. Among them, *EGFR* was associated with tumorigenesis, and *PEX5*, *PLCG2*, and *PRKCD* were associated with immune processes. Thus, convergent signatures in more than 11 genes related to cancer progression—four positively selected genes and seven genes with convergent amino acid changes—were found in two or more long-lived lineages, suggesting that long-lived mammals might have evolved convergent or similar mechanisms for cancer resistance in response to increased longevity.

Evolution of longevity through cancer resistance

The risk of cancer is a major challenge for increasing lifespan in mammals. Previous studies have shown that long-lived mammals have evolved specific mechanisms to protect themselves from cancer invasion. For instance, the two longest-living subterranean rodent species, the naked mole rat and blind mole rat, were found to resist cancer by secreting high-molecular-mass hyaluronan to mediate early contact inhibition and by using interferon secretion to induce cell death, respectively.[42,43]

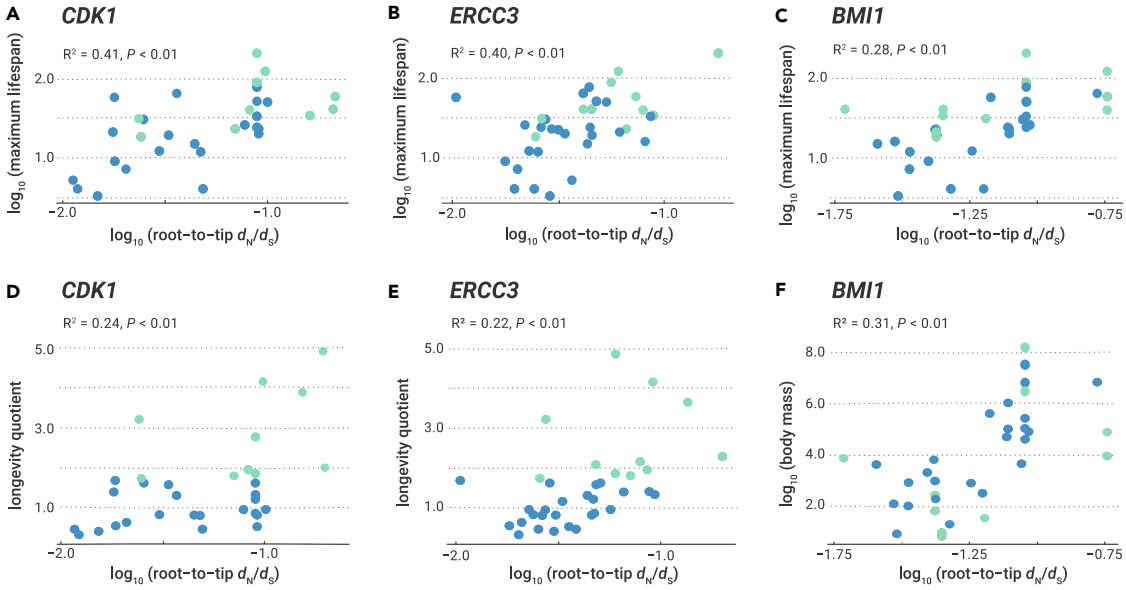

Figure 3. Root-to-tip d_N/d_S values of genes with significant correlation with three life-history traits Scatterplots of significant relationships between $\log_{10}$ (maximum lifespan) (A–C), $\log_{10}$ (body mass) (F), longevity quotient (D and E), and root-to-tip d_N/d_S values. Green and blue points represent long-lived and control species, respectively.

Most notably, the tumor-suppressing TP53 gene might function differently in blind mole rats and another group of long-lived species, elephants. It was found that an amino acid change in the p53 protein of blind mole rats (R174K in human) favors cell-cycle arrest over apoptosis to adapt to the rat's hypoxic subterranean environment.[44] However, massive expansion of the many copies of TP53 identified in elephants was suggested to increase cellular sensitivity to DNA damage by triggering p53-dependent apoptosis, which leads to efficient removal of mutant cells.[14]

Previous studies have also shown that many genes related to cancer control (including DNA damage and repair, immune response, and tumor suppression) evolved under positive selection, duplication, and amino acid changes in several long-lived lineages, suggesting that they share a mechanism. Positive selection of the pro-apoptotic gene *FOXO3* and tumor-suppressor gene *PRDM1* (positive regulatory domain I), and the specific mutation of the DNA-repair enzymes ERCC1 (excision repair cross-complementation group 1) was identified in long-lived bowhead and humpback whales;[12,13]

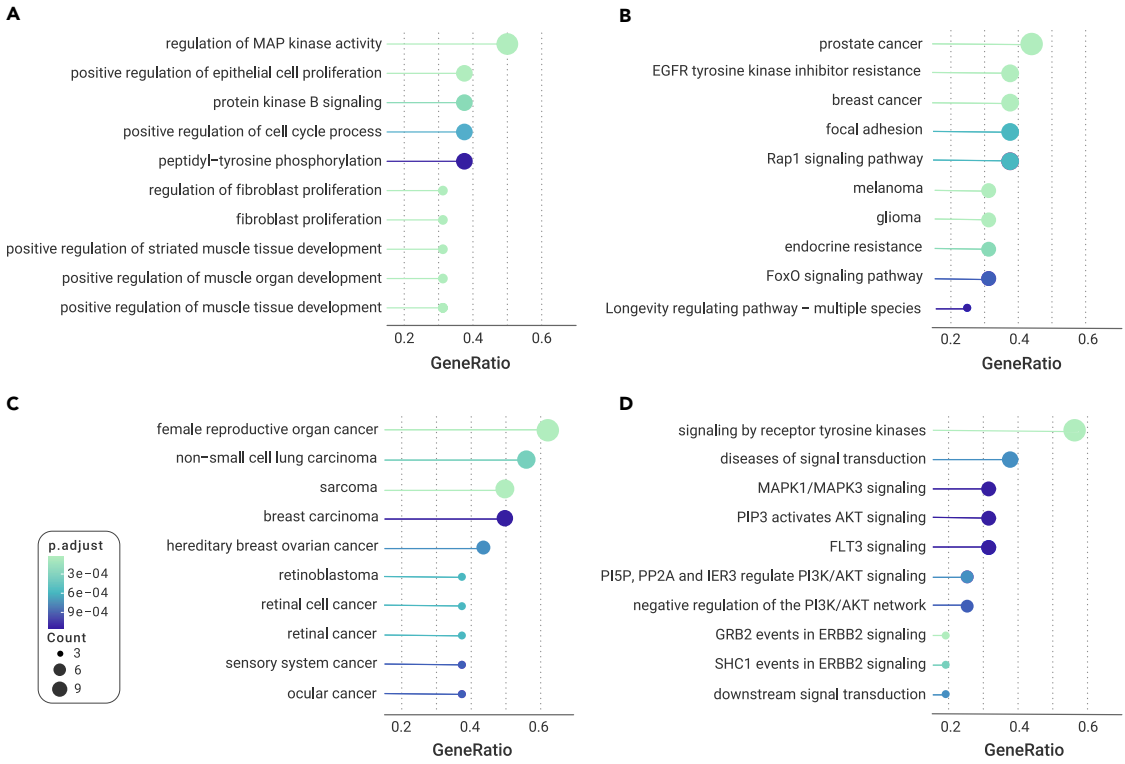

Figure 4. Pathway enrichment of genes with significant correlation with longevity-associated traits Enriched (A) GO terms, (B) KEGG pathways, (C) DO terms, and (D) Reactome pathways of genes correlate with the longevity-associated traits (i.e., maximum lifespan, longevity quotient, and body mass). Only the top ten terms are shown. Circle sizes are proportional to the number of genes assigned to a pathway, and the color of the circle indicates the adjusted p value for each pathway.

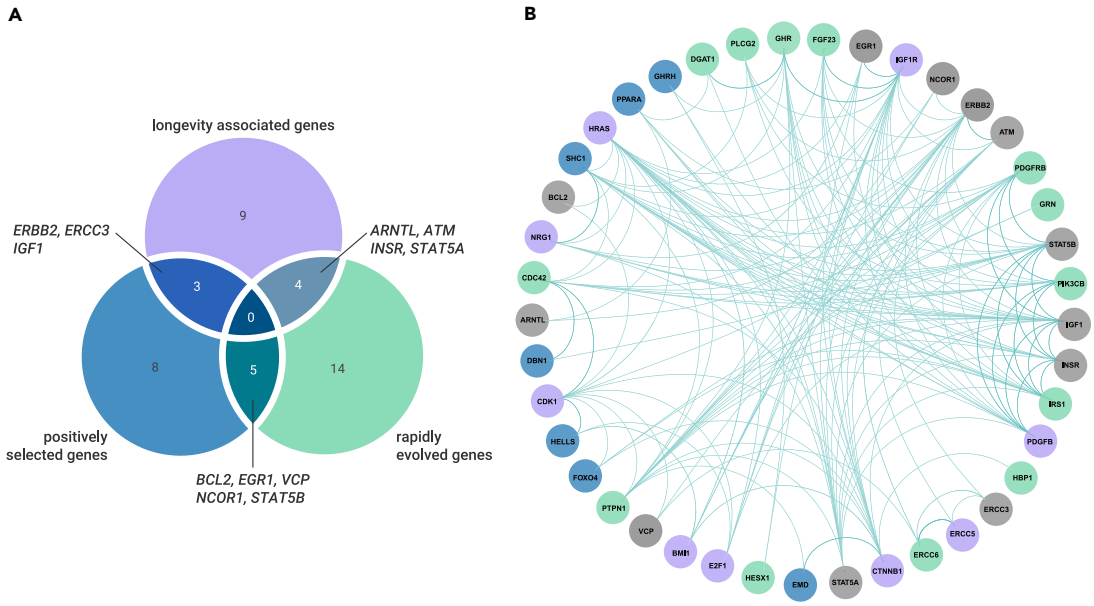

Figure 5. Overview of 12 robust longevity-associated genes (A) Venn diagram of overlaps among positively selected genes, longevity-associated genes, and rapidly evolving genes. (B) Protein-protein interaction network generated using STRING. Nodes for positively selected genes, longevity-associated genes, rapidly evolving genes, and overlap genes are colored blue, purple, green, and gray, respectively. Lines between each node indicate inferred/experimentally demonstrated biological associations.

on the other hand, in blind mole rats and microbats, inflammation-regulation-related genes (e.g., Ifnb1, Mx1, and c-REL) showed positive selection, and gene families involved in immune response underwent gene expansion.[34]

In our study, 12 robust candidates for longevity-related genes identified in the long-lived lineages were involved in DNA repair (*ERCC3* and *ATM*), immune processes (*BCL2*, *STAT5A*, *STAT5B*, and *VCP*), and the IIS pathway (*IGF1* and *INSR*). Interestingly, 8 of these 12 candidates are known cancer genes according to the COSMIC v92[45] and TSGene 2.0[46] databases: five tumor-suppressor genes (*ATM*, *EGR1*, *IGF1*, *STAT5A*, and *NOCR1*); two oncogenes (*BCL2* and *ERBB2*); and *STAT5B*, which is classified as both a tumor-suppressor gene and an oncogene. For example, *EGR1* (early growth response 1), detected to be under positive selection in the long-lived Sumatran orangutan, upregulates the expression of TP53 to induce apoptosis in cancer cells.[47] *STAT5B* (signal transducer and activator of transcription 5B), identified to be under positive selection and rapid evolution in the long-lived lineages, has been shown to activate STAT5, which is associated with the suppression of antitumor immunity and an increase in the proliferation, invasion, and survival of tumor cells.[48] *ATM* is a key DNA-damage response gene that commonly mutates in cancer; it functions as a regulator of a wide variety of downstream proteins, including the tumor-suppressor proteins TP53 and BRCA1.[49] Similarly, *ATM* was also identified to be under positive selection in the genus *Myotis*.[50] As mentioned above, a number of genes involved in cancer-related pathways have evolved via the same or different evolutionary pathways in individual or multiple long-lived lineages, suggesting that cancer resistance could be achieved through lineage-specific adaptations or common mechanisms to extend lifespan. Of course, functional experiments are needed to test whether the candidate cancer-related genes have higher cancer-resistance activity in the long-lived mammals compared with short-lived counterparts; such experiments are important in part because they may provide new strategies to extend the lifespan of humans.

Conclusion

The striking variability in lifespans across the mammalian phylogeny provides an ideal dataset to investigate the evolution of extended lifespan (longevity) and aging. Using mammalian comparative genomics, we juxtaposed 11 long-lived species with 25 shorter-lived counterparts. Our findings support our hypothesis that the IIS pathway and immune regulation play a particularly important role in exceptional mammalian longevity. Eleven cancer-related genes were found to have convergent signatures in the long-lived species, indicating functional convergence or similar anticancer mechanisms in response to increased longevity in animals. Importantly, we identified 12 robust candidates for longevity-related genes that were closely related to cancer, which corroborated the notion that long-lived mammals have evolved effective anticancer mechanisms to extend their lifespan. Together, these findings provide insights into how evolution reversibly adjusts lifespan and presents candidate genes and pathways for further experimental exploration.

MATERIALS AND METHODS

See supplemental information for details.

REFERENCES

1. Tacutu, R., Thornton, D., Johnson, E., et al. (2018). Human aging genomic resources: new and updated databases. Nucleic Acids Res. ***46***, D1083–D1090.
2. Tollis, M., Boddy, A.M., and Maley, C.C. (2017). Peto's Paradox: how has evolution solved the problem of cancer prevention? BMC Biol. ***15***, 1–5.
3. John, C., and Bockstoce, J.R. (2008). Two historical weapon fragments as an aid to estimating the longevity and movements of bowhead whales. Polar Biol. ***31***, 751–754.
4. George, J.C., Bada, J., Zeh, J., et al. (1999). Age and growth estimates of bowhead whales (Balaena mysticetus) via aspartic acid racemization. Can. J. Zool. ***77***, 571–580.
5. Wiese, R.J., and Willis, K. (2004). Calculation of longevity and life expectancy in captive elephants. Zoo Biol. ***23***, 365–373.
6. Podlutsky, A.J., Khritankov, A.M., Ovodov, N.D., and Austad, S.N. (2005). A new field record for bat longevity. J. Gerontol. A Biol. Sci. Med. Sci. ***60***, 1366–1368.
7. Kim, E.B., Fang, X., Fushan, A.A., et al. (2011). Genome sequencing reveals insights into physiology and longevity of the naked mole rat. Nature ***479***, 223–227.
8. Buffenstein, R. (2008). Negligible senescence in the longest living rodent, the naked mole-rat: insights from a successfully aging species. J. Comp. Physiol. B ***178***, 439–445.
9. Holmes, D.J., and Austad, S.N. (1994). Fly now, die later: life-history correlates of gliding and flying in mammals. J. Mammal. ***75***, 224–226.
10. Austad, S. (2010). Methusaleh's Zoo: how nature provides us with clues for extending human health span. J. Comp. Pathol. ***142***, S10–S21.
11. López-Otín, C., Blasco, M.A., Partridge, L., et al. (2013). The hallmarks of aging. Cell ***153***, 1194–1217.
12. Tollis, M., Robbins, J., Webb, A.E., et al. (2019). Return to the sea, get huge, beat cancer: an analysis of cetacean genomes including an assembly for the humpback whale (*Megaptera novaeangliae*). Mol. Biol. Evol. ***36***, 1746–1763.

13. Keane, M., Semeiks, J., Webb, A.E., et al. (2015). Insights into the evolution of longevity from the bowhead whale genome. Cell Rep. ***10***, 112–122.
14. Sulak, M., Fong, L., Mika, K., et al. (2016). TP53 copy number expansion is associated with the evolution of increased body size and an enhanced DNA damage response in elephants. eLife ***5***, e11994.
15. Seim, I., Fang, X., Xiong, Z., et al. (2013). Genome analysis reveals insights into physiology and longevity of the Brandt's bat *Myotis brandtii*. Nat. Commun. ***4***, 1–8.
16. Tian, X., Azpurua, J., Hine, C., et al. (2013). High-molecular-mass hyaluronan mediates the cancer resistance of the naked mole rat. Nature ***499***, 346–349.
17. MacRae, S.L., Croken, M.M., Calder, R., et al. (2015). DNA repair in species with extreme lifespan differences. Aging (Albany NY) ***7***, 1171.
18. De Magalhães, J.P., and Toussaint, O. (2004). GenAge: a genomic and proteomic network map of human aging. FEBS Lett. ***571***, 243–247.
19. De Magalhães, J.P., Costa, J., and Church, G.M. (2007). An analysis of the relationship between metabolism, developmental schedules, and longevity using phylogenetic independent contrasts. J. Gerontol. A Biol. Sci. Med. Sci. ***62***, 149–160.
20. Charnov, E.L. (1993). Life History Invariants: Some Explorations of Symmetry in Evolutionary Ecology (Oxford University Press).
21. De Magalhães, J.P., and Church, G.M. (2007). Analyses of human-chimpanzee orthologous gene pairs to explore evolutionary hypotheses of aging. Mech. Aging Dev. ***128***, 355–364.
22. De Magalhães, J.P., and Costa, J. (2009). A database of vertebrate longevity records and their relation to other life-history traits. J. Evol. Biol. ***22***, 1770–1774.
23. Kenyon, C. (2011). The first long-lived mutants: discovery of the insulin/IGF-1 pathway for aging. Philos. Trans. R. Soc. Lond. B Biol. Sci. ***366***, 9–16.
24. Selman, C., Lingard, S., Choudhury, A.I., et al. (2008). Evidence for lifespan extension and delayed age-related biomarkers in insulin receptor substrate 1 null mice. FASEB J. ***22***, 807–818.
25. Blüher, M., Kahn, B.B., and Kahn, C.R. (2003). Extended longevity in mice lacking the insulin receptor in adipose tissue. Science ***299***, 572–574.
26. Shimokawa, I., Higami, Y., Utsuyama, M., et al. (2002). Life span extension by reduction in growth hormone-insulin-like growth factor-1 axis in a transgenic rat model. Am. J. Pathol. ***160***, 2259–2265.
27. Holzenberger, M., Dupont, J., Ducos, B., et al. (2003). IGF-1 receptor regulates lifespan and resistance to oxidative stress in mice. Nature ***421***, 182–187.
28. David, A., Hwa, V., Metherell, L.A., et al. (2011). Evidence for a continuum of genetic, phenotypic, and biochemical abnormalities in children with growth hormone insensitivity. Endocr. Rev. ***32***, 472–497.
29. Ikeno, Y., Hubbard, G.B., Lee, S., et al. (2009). Reduced incidence and delayed occurrence of fatal neoplastic diseases in growth hormone receptor/binding protein knockout mice. J. Gerontol. A. Biol. Sci. Med. Sci. ***64***, 522–529.
30. Guevara-Aguirre, J., Balasubramanian, P., Guevara-Aguirre, M., et al. (2011). Growth hormone receptor deficiency is associated with a major reduction in pro-aging signaling, cancer, and diabetes in humans. Sci. Transl. Med. ***3***, 70ra13.
31. Ma, S., Upneja, A., Galecki, A., et al. (2016). Cell culture-based profiling across mammals reveals DNA repair and metabolism as determinants of species longevity. eLife ***5***, e19130.
32. Wang, D., Feng, J., Wen, R., et al. (2000). Phospholipase Cγ2 is essential in the functions of B cell and several Fc receptors. Immunity ***13***, 25–35.
33. Barreiro, L.B., and Quintana-Murci, L. (2010). From evolutionary genetics to human immunology: how selection shapes host defence genes. Nat. Rev. Genet. ***11***, 17–30.
34. Ma, S., and Gladyshev, V.N. (2017). Molecular signatures of longevity: insights from cross-species comparative studies. Semin. Cell Dev. Biol. ***70***, 190–203.
35. Fushan, A.A., Turanov, A.A., Lee, S.G., et al. (2015). Gene expression defines natural changes in mammalian lifespan. Aging Cell ***14***, 352–365.
36. Valenzano, D.R., Benayoun, B.A., Singh, P.P., et al. (2015). The African turquoise killifish genome provides insights into evolution and genetic architecture of lifespan. Cell ***163***, 1539–1554.
37. Xie, Y., Shi, X., Sheng, K., et al. (2019). PI3K/Akt signaling transduction pathway, erythropoiesis and glycolysis in hypoxia. Mol. Med. Rep. ***19***, 783–791.
38. Hao, Y., Qu, Y., Song, G., and Lei, F. (2019). Genomic insights into the adaptive convergent evolution. Curr. Genomics ***20***, 81–89.
39. Khatri, A., Wang, J., and Pendergast, A.M. (2016). Multifunctional Abl kinases in health and disease. J. Cell. Sci. ***129***, 9–16.
40. Östman, A., and Heldin, C.H. (2007). PDGF receptors as targets in tumor treatment. Adv. Cancer Res. ***97***, 247–274.
41. Wils, H., Kleinberger, G., Pereson, S., et al. (2012). Cellular aging, increased mortality and FTLD-TDP-associated neuropathology in progranulin knockout mice. J. Pathol. ***228***, 67–76.
42. Gorbunova, V., Hine, C., Tian, X., et al. (2012). Cancer resistance in the blind mole rat is mediated by concerted necrotic cell death mechanism. Proc. Natl. Acad. Sci. U S A ***109***, 19392–19396.
43. Delaney, M., Nagy, L., Kinsel, M., and Treuting, P. (2013). Spontaneous histologic lesions of the adult naked mole rat (*Heterocephalus glaber*): a retrospective survey of lesions in a zoo population. Vet. Pathol. ***50***, 607–621.
44. Ashur-Fabian, O., Avivi, A., Trakhtenbrot, L., et al. (2004). Evolution of p53 in hypoxia-stressed *Spalax* mimics human tumor mutation. Proc. Natl. Acad. Sci. U S A ***101***, 12236–12241.
45. Tate, J.G., Bamford, S., Jubb, H.C., et al. (2019). COSMIC: the catalogue of somatic mutations in cancer. Nucleic Acids Res. ***47***, D941–D947.
46. Zhao, M., Kim, P., Mitra, R., et al. (2016). TSGene 2.0: an updated literature-based knowledgebase for tumor suppressor genes. Nucleic Acids Res. ***44***, D1023–D1031.
47. Yu, J., Baron, V., Mercola, D., et al. (2007). A network of p73, p53 and Egr1 is required for efficient apoptosis in tumor cells. Cell Death Differ. ***14***, 436–446.
48. Rani, A., and Murphy, J.J. (2016). STAT5 in cancer and immunity. J. Interferon Cytokine Res. ***36***, 226–237.
49. Weber, A.M., and Ryan, A.J. (2015). ATM and ATR as therapeutic targets in cancer. Pharmacol. Ther. ***149***, 124–138.
50. Foley, N.M., Hughes, G.M., et al. (2018). Growing old, yet staying young: the role of telomeres in bats' exceptional longevity. Sci. Adv. ***4***, eaao0926.

ACKNOWLEDGMENTS

This study was supported by the National Natural Science Foundation of China (NSFC, grant nos. 32070409, 31772448 to S.X., 31872219 to W.R.), the Key Project of the NSFC (grant nos. 32030011, 31630071 to G.Y.), National Key Programme of Research and Development of China, Ministry of Science and Technology (grant no. 2016YFC0503200 to G.Y. and S.X.), the Priority Academic Program Development of Jiangsu Higher Education Institutions to G.Y. and S.X., and the Qinglan project of Jiangsu Province to S.X. These funding bodies played no role in study design, data collection, analysis, interpretation of data, and writing the manuscript. We are particularly grateful to Dr. Yan-bo Sun (Yunnan University, Kunming, Yunnan, China) for the suggestion of data analysis. Many thanks are also given to Zepeng Zhang, Simin Chai, Yuan Mu, and Weijian Guo for support and discussions.

AUTHOR CONTRIBUTIONS

S.X. and G.Y. designed the study. Z.Y. was responsible for data collection and analysis. S.X. and Z.Y. drafted the manuscript. I.S., S.X., and G.Y. revised the manuscript. M.Y. participated in data collection. D.S. contributed to data analysis. R.T. and W.R. assisted with manuscript editing. All authors read and approved the final manuscript.

DECLARATION OF INTERESTS

The authors declare no competing interests.

LEAD CONTACT WEBSITE

http://sky.njnu.edu.cn/cn/shiziduiwu/xu-shi-xia.

SUPPLEMENTAL INFORMATION

Supplemental information can be found online at https://doi.org/10.1016/j.xinn.2021.100108.

The Innovation, Volume *2*

Supplemental Information

Comparative analyses of aging-related genes in long-lived mammals provide insights into natural longevity

Zhenpeng Yu, Inge Seim, Mengxin Yin, Ran Tian, Di Sun, Wenhua Ren, Guang Yang, and Shixia Xu

Supplementary Information

Comparative analyses of aging-related genes in long-lived mammals provide insights into natural longevity

Zhenpeng Yu,[1] Inge Seim,[1,2,3] Mengxin Yin,[1] Ran Tian,[1] Di Sun,[1] Wenhua Ren,[1] Guang Yang,[1,*] and Shixia Xu[1,*]

[1] Jiangsu Key Laboratory for Biodiversity and Biotechnology, College of Life Sciences, Nanjing Normal University, Nanjing 210023, China

[2] Integrative Biology Laboratory, College of Life Sciences, Nanjing Normal University, Nanjing 210023, China

[3] School of Biology and Environmental Science, Faculty of Science and Engineering, Queensland University of Technology, Brisbane, QLD, Australia

[*]Correspondence: gyang@njnu.edu.cn (G.Y.); xushixia78@163.com (S.X.)

MATERIALS AND METHODS

Species Coverage and Definition of Long-lived Species

A total of 36 mammals representing 14 orders were examined: Cetartiodactyla (*B. mysticetus, Tursiops truncates, Orcinus orca, Lipotes vexillifer, Balaenoptera acutorostrata, Physeter catodon, Neophocaena asiaeorientalis, Vicugna pacos, Bos Taurus, Ovis aries*), Perissodactyla (*Equus caballus*), Carnivora (*Canis lupus familiaris, Felis catus*), Chiroptera (*M. brandtii, Myotis lucifugus, Pteropus vampyrus*), Eulipotyphla (*Sorex araneus, Erinaceus europaeus*), Primates (*H. sapiens, M. nemestrina, Carlito syrichta, P. abelii, C. jacchus, M. murinus*), Rodentia (*H. glaber, Rattus norvegicus, Mus musculus, Cavia porcellus*), Lagomorpha (*Oryctolagus cuniculus, Ochotona princeps*), Proboscidea (*L. Africana*) , Hyracoidea (*Procavia capensis*), Afrosoricida (*Echinops telfairi*), Cingulata (*Dasypus novemcinctus*), Pilosa (*Choloepus hoffmanni*), and Didelphimorphia (*Monodelphis domestica*) (Table S1).

We used the scientific method of evaluating longevity quotient (LQ)—i.e., the ratio of the observed maximum lifespan (MLS) to the predicted maximum lifespan[1-2]—to determine whether species are long-lived for their body size. We first obtained the maximum lifespan and body mass (BM) records for all mammals (n = 987) from the AnAge online database.[3] Each species' longevity quotient was calculated to follow the allometric equation for mammals:[2]

$$LQ = \frac{MLS}{6.32 \times BM^{0.139}}$$

Then, we split the dataset into two groups based on longevity quotient: long-lived group contained the species with a longevity quotient greater than 1 SD (standard

deviation) from the mean of all mammals, and the control group contained all other species.

Sequence Retrieval and Alignments

Aging-related gene list of human was first retrieved from the GenAge[3] database. The protein-coding sequence (CDS) for each human aging-related gene was then downloaded from the NCBI database. The CDS of other mammalian species was downloaded from NCBI, the OrthoMAM v10 database,[4] and the Bowhead Whale Genome Resource (http://www.bowhead-whale.org/).[5] Additionally, the low quality or unannotated CDS in the database was further verified using BLASTn searches. For each gene, the longest transcript was kept in our analysis. Thus, 115 one-to-one orthologous genes among 36 species were selected for subsequent analysis (Table S2). Next, we performed multiple sequence alignments for each orthologous gene using PRANK with default settings, which uses phylogenetic information to distinguish alignment gaps caused by insertions or deletions and produces good alignments for evolutionary inferences.[6-7] Finally, potentially unreliable regions of multiple alignments were removed using the Gblocks v0.91 program with default settings ("-t = c").[8]

Molecular Evolution Analyses

The measure of natural selection acting on the genes was determined by estimating the ratio of nonsynonymous (d_N) / synonymous (d_S) substitution rates (d_N/d_S) implemented in the CodeML program of the PAML software package v4.9.[9] Briefly,

$d_N/d_S < 1$, $d_N/d_S = 1$, and $d_N/d_S > 1$ indicate negative selection, neutral evolution, and positive selection, respectively. A well-accepted species tree of 36 species in our study from the TimeTree database (http://www.timetree.org/) was used as the input tree for all analyses.[10]

To investigate whether aging-related genes have undergone significant differences in selection pressures between long-lived species and the control group, the branch-site model was used to test the selection of each extant lineage in this study.[11] Each long-lived species was used as a foreground branch in every run, and all control group species were set as the background branch. Compared with the null hypothesis model of neutral evolution ($d_N/d_S = 1$), foreground branches in the modified model A that have a class of sites with the ratio $d_N/d_S > 1$ for positive selection. All positively selected sites in the branch-site model were identified using a Bayes Empirical Bayes (BEB) analysis with posterior probabilities $\geqslant 0.80$.[12] In addition, the clade model C and its null model M2a_rel (nearly neutral) were used to detect evidence of divergent selective pressures acting across the combined branch of all extant long-lived lineage as the foreground compared with the remaining species in the tree as the background.[13] The clade model C assumes variation in d_N/d_S among sites, allowing a fraction of sites evolving under divergent selective pressures. The model assumes three classes of sites, representing evolutionarily conserved codons, neutral codons, and codons under divergent selection pressures between the foreground and background clades. We set each model with three initial d_N/d_S values (0.5, 1, and 1.5) to obtain the robust average d_N/d_S, and compared this result with that of model M2a_ref. Only genes with an unchangeable likelihood

value for the three initial d_N/d_S values were considered. The likelihood ratio test (LRT) with χ^2 distribution was used to determine which models were statistically different from the null model. The *P*-values were adjusted for multiple testing using the false discovery rate (FDR) procedure and adjusted *P*-values < 0.05 were considered significant for branch-site model analysis.[14]

Convergent Evolution Detection

Here, we used two methods to detect the molecular basis of convergent evolution in long-lived species. First, ancestral amino acid sequences were reconstructed for 115 one-to-one orthologous genes among 36 species using the CodeML program in PAML 4.9.[9] Then, convergent amino acid substitutions in independent pairs of long-lived lineage were detected by Zhang and Kumar's method.[15] Considering noise resulting from the random amino acid substitutions of convergence, the JTT-f_{genes} model of amino acid substitution were used to estimate the expected number of molecular convergences in each protein alignment.[16] A Poisson test was finally performed to verify whether the observed number of convergent sites in each gene was significantly more than the expected number caused by random substitution.

Second, we determined unique amino acid substitutions based on sequence alignments using FasParser2,[17] since convergent phenotypic characteristics can also arise from unique substitutions that independently evolved in different species.[18] If the same amino acid changes were identified in at least five long-lived species and none were found in the control group, then these amino acid changes were considered to be

long-lived group specific amino acid substitutions.

Association Analysis between Gene Evolution and Phenotypes

Finally, we wished to assess the relationship between the rate of gene evolution and aging-associated life-history traits.[19] To test whether maximum lifespan covaries with body mass and longevity quotient, we first carried out a nonphylogenetic regression using the *lm* function in R 3.5.1. Moreover, we used Pagel's λ model to test for phylogenetic signals in mammalian life-history traits. Pagel's λ describes the proportion of variance that can be attributed to Brownian motion along a phylogeny. A value of λ equal or close to 1 suggests that the character is evolving stochastically, whereas $\lambda < 1$ indicates a departure from neutral drift. Estimates of λ for all life-history traits were computed using the *phytools* package in R 3.5.1.[20]

To explore the potential relationships between the evolutionary rate (d_N / d_S) of aging-related genes and life-history phenotypes, the root-to-tip d_N / d_S that considers the evolutionary history of a locus were calculated for each gene using the free-ratio model from PAML v4.9.[9] For this analysis, a d_S value of approximately 0 along a branch always yields a very high d_N/d_S value. Hence, genes with $d_S < 0.0001$ were discarded in our analysis. Finally, phylogenetic generalized least squares regression was performed in the *caper* package in R 3.5.1[21] to evaluate the associations between Log_{10}-transformed root-to-tip d_N/d_S and life-history traits (longevity quotient without log-transform).[22]

To assess the robustness of the results, we applied a two-step verification

procedure as previously described.[23] First, the regression was performed by excluding the species with the largest residue error (e.g., a potential outlier) to report the regression slope *P*-value ("*P* value.robust"). Second, the regression was repeated by excluding each species, one at a time, to report the maximum (i.e., least significant) *P*-value ("*P* value.max"), and ensure that the overall relationship did not depend on any single species. Both *P* value.robust < 0.01 and *P* value.max < 0.1 were chosen as the cut-offs.

Pathway Enrichment and Protein-protein Interaction Analysis

We performed a pathway enrichment analysis to explore the biological mechanisms underlying the associations between the candidate genes and longevity pathways. The functional enrichment analyses in Gene Ontology (GO) terms for Biological Process (BP), the Kyoto Encyclopedia of Genes and Genomes (KEGG), Disease Ontology (DO), and Reactome pathway were performed in the R package *clusterProfiler*.[24] DO provides a consistent description of genes in disease perspectives and Reactome is a manually curated resource that describes chemical reactions and biological processes and pathways. For each pathway, the hypergeometric test was used to detect any overrepresentation of our set of genes among all genes in the pathway. FDR was controlled using the Benjamini–Hochberg procedure in R 3.5.1.[25] A protein-protein interaction network analysis was performed using STRING v11.[26]

Supplementary Figure

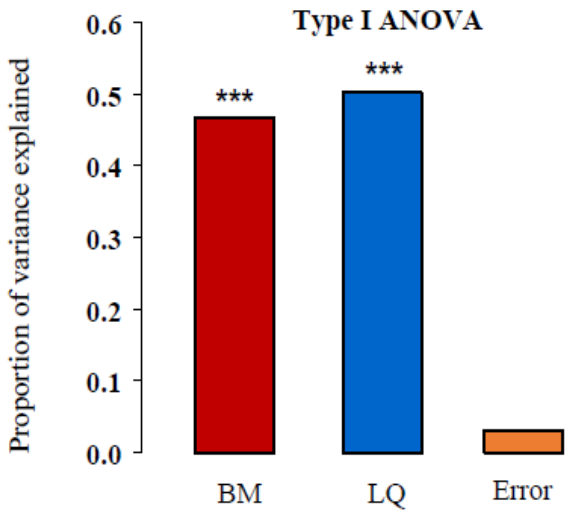

Figure S1. Bar plot showing the variance in maximum lifespan (MLS) explained by each life-history trait (body mass (BM) or longevity quotient (LQ)) as studied in a multivariate model, ***P value < 0.001.

Supplementary Tables

Table S1 Datasets of 36 mammals in the present study.

Order	Species	MLS/year	BM/g	LQ
Cetartiodactyla	*Balaena mysticetus*	211	100,000,000	2.58
	Tursiops truncatus	51.6	200,000	1.50
	Orcinus orca	90	3,987,500	1.72
	Lipotes vexillifer	24	83,500	0.79
	Balaenoptera acutorostrata	50	7,500,000	0.88
	Physeter catodon	77	28,500,000	1.12
	Neophocaena asiaeorientalis	33	32,500	1.23
	Vicugna pacos	25.8	62,000	0.88
	Bos taurus	20	750,000	0.48
	Ovis aries	22.8	80,000	0.75
Perissodactyla	*Equus caballus*	57	300,000	1.56
Carnivora	*Canis lupus familiaris*	24	40,000	0.87
	Felis catus	30	3,900	1.50
Chiroptera	*Myotis brandtii*	41	7	4.95
	Myotis lucifugus	34	10	3.91
	Pteropus vampyrus	20.9	872	1.29
Eulipotyphla	*Sorex araneus*	3.2	9	0.37
	Erinaceus europaeus	11.7	750	0.74
Primates	*Homo sapiens*	122.5	62,035	4.18
	Macaca nemestrina	37.6	7,913	1.71
	Carlito syrichta	16	119.2	1.30
	Pongo abelii	59	64,475	2.00
	Callithrix jacchus	22.8	255.2	1.67
	Microcebus murinus	18.2	64.8	1.61
Rodentia	*Heterocephalus glaber*	31	35	2.99
	Rattus norvegicus	3.8	300	0.27
	Mus musculus	4	20.5	0.42
	Cavia porcellus	12	728	0.76
Lagomorpha	*Oryctolagus cuniculus*	9	1,800	0.50
	Ochotona princeps	7	100	0.58
Afrotheria	*Loxodonta africana*	65	4,800,000	1.21
	Procavia capensis	14.8	3,600	0.75
	Echinops telfairi	19	180	1.46
Cingulata	*Dasypus novemcinctus*	22.3	5,500	1.07
Pilosa	*Choloepus hoffmanni*	41	6,250	1.93
Didelphimorphia	*Monodelphis domestica*	5.1	105	0.42

Table S2 List of 115 aging-related genes used in in the present study.

Gene	Entrez ID	Gene Name	Gene Function/GeneCards
ABL1	25	ABL proto-oncogene 1, non-receptor tyrosine kinase	Cancer
AGTR1	185	angiotensin II receptor, type 1	Metabolism
APOE	348	apolipoprotein E	Metabolism
APP	351	amyloid beta precursor protein	Transcription regulation
APTX	54840	aprataxin	DNA damage repair
ARNTL	406	aryl hydrocarbon receptor nuclear translocator-like	Transcription regulation
ATF2	1386	activating transcription factor 2	Transcription regulation
ATM	472	ATM serine/threonine kinase	Cancer
ATP5O	539	ATP synthase peripheral stalk subunit OSCP	Metabolism
ATR	545	ATR serine/threonine kinase	Cancer
BAX	581	BCL2-associated X protein	Apoptosis
BCL2	596	B-cell CLL/lymphoma 2	Apoptosis
BLM	641	Bloom syndrome, RecQ helicase-like	DNA damage repair
BMI1	648	BMI1 proto-oncogene, polycomb ring finger	DNA damage repair
BRCA1	672	breast cancer 1, early onset	Cancer
BSCL2	26580	Berardinelli-Seip congenital lipodystrophy 2	Immune system
BUB3	9184	BUB3 mitotic checkpoint protein	Cell cycle
C1QA	712	complement component 1, q subcomponent, A chain	Cell cycle
CCNA2	890	cyclin A2	Cell cycle
CDC42	998	cell division cycle 42	Cell cycle
CDK1	983	cyclin-dependent kinase 1	Cell cycle

CDK7	1022	cyclin-dependent kinase 7	Cell cycle
CDKN1A	1026	cyclin-dependent kinase inhibitor 1A	Cell cycle
CDKN2B	1030	cyclin-dependent kinase inhibitor 2B	Cell cycle
CHEK2	11200	checkpoint kinase 2	Cell cycle
CISD2	493856	CDGSH iron sulfur domain 2	Apoptosis
CLOCK	9575	clock circadian regulator	Transcription regulation
CNR1	1268	cannabinoid receptor 1 (brain)	Cell Surface Receptors
COQ7	10229	coenzyme Q7 homolog, ubiquinone (yeast)	Metabolism
CREB1	1385	cAMP responsive element binding protein 1	Transcription regulation
CREBBP	1387	CREB binding protein	Transcription regulation
CSNK1E	1454	casein kinase 1, epsilon	DNA damage repair
CTGF	1490	connective tissue growth factor	Growth regulation
CTNNB1	1499	catenin (cadherin-associated protein), beta 1	Signal transduction
DBN1	1627	drebrin 1	Signal transduction
DGAT1	8694	diacylglycerol O-acyltransferase 1	Metabolism
E2F1	1869	E2F transcription factor 1	Apoptosis
EFEMP1	2202	EGF containing fibulin-like extracellular matrix protein 1	Growth regulation
EGFR	1956	epidermal growth factor receptor	Cancer
EGR1	1958	early growth response 1	Growth regulation
EIF5A2	56648	eukaryotic translation initiation factor 5A2	Transcription regulation
EMD	2010	emerin	Growth regulation
EPOR	2057	Erythropoietin receptor	Growth regulation
EPS8	2059	epidermal growth factor receptor pathway substrate 8	Growth regulation
ERBB2	2064	erb-b2 receptor tyrosine kinase 2	Cancer

ERCC1	2067	excision repair cross-complementation group 1	DNA damage repair
ERCC2	2068	excision repair cross-complementation group 2	DNA damage repair
ERCC3	2071	excision repair cross-complementation group 3	DNA damage repair
ERCC5	2073	excision repair cross-complementation group 5	DNA damage repair
ERCC6	2074	excision repair cross-complementation group 6	DNA damage repair
ERCC8	1161	excision repair cross-complementation group 8	DNA damage repair
ESR1	2099	estrogen receptor 1	Growth regulation
FGF23	8074	fibroblast growth factor 23	Growth regulation
FGFR1	2260	fibroblast growth factor receptor 1	Growth regulation
FOS	2353	FBJ murine osteosarcoma viral oncogene homolog	Transcription regulation
FOXM1	2305	forkhead box M1	Cell cycle
FOXO1	2308	forkhead box O1	Transcription regulation
FOXO3	2309	forkhead box O3	Transcription regulation
FOXO4	4303	forkhead box O4	Transcription regulation
GCLC	2729	glutamate-cysteine ligase, catalytic subunit	Growth regulation
GCLM	2730	glutamate-cysteine ligase, modifier subunit	Growth regulation
GHR	2690	growth hormone receptor	Growth regulation
GHRH	2691	growth hormone releasing hormone	Growth regulation
GRB2	2885	growth factor receptor-bound protein 2	Signal transduction
GRN	2896	granulin	Growth regulation
GSK3B	2932	glycogen synthase kinase 3 beta	Metabolism
GSS	2937	glutathione synthetase	Metabolism
GSTA4	2941	glutathione S-transferase alpha 4	Metabolism
GTF2H2	2966	general transcription factor IIH, polypeptide 2	DNA damage repair

H2AFX	3014	H2A histone family, member X	DNA damage repair
HBP1	26959	HMG-box transcription factor 1	Transcription regulation
HDAC3	8841	histone deacetylase 3	Transcription regulation
HELLS	3070	helicase, lymphoid-specific	DNA damage repair
HESX1	8820	HESX homeobox 1	Transcription regulation
HIF1A	3091	hypoxia inducible factor 1, alpha subunit	Metabolism
HMGB1	3146	high mobility group box 1	DNA damage repair
HMGB2	3148	high mobility group box 2	DNA damage repair
HRAS	3265	Harvey rat sarcoma viral oncogene homolog	Cancer
IGF1	3479	insulin-like growth facto 1	Growth regulation
IGF1R	3480	insulin-like growth factor 1 receptor	Growth regulation
IL2	3558	interleukin 2	Immune system
IL2RG	3561	interleukin 2 receptor, gamma	Immune system
IL7R	3575	interleukin 7 receptor	Immune system
INSR	3643	insulin receptor	Growth regulation
IRS1	3667	insulin receptor substrate 1	Signal transduction
LMNA	4000	lamin A/C	Growth regulation
NCOR1	9611	nuclear receptor corepressor 1	Transcription regulation
NGF	4803	nerve growth factor	Signal transduction
NGFR	4804	nerve growth factor receptor	Signal transduction
NRG1	3084	neuregulin 1	Growth regulation
PDGFB	5155	platelet-derived growth factor beta polypeptide	Growth regulation
PDGFRB	5159	platelet-derived growth factor receptor, beta polypeptide	Growth regulation
PEX5	5830	peroxisomal biogenesis factor 5	Metabolism

PIK3CB	5291	phosphatidylinositol-4,5-bisphosphate 3-kinase, catalytic subunit beta	Signal transduction
PIN1	5300	peptidylprolyl cis/trans isomerase, NIMA-interacting 1	Cell cycle
PLAU	5328	plasminogen activator, urokinase	Signal transduction
PLCG2	5336	phospholipase C, gamma 2	Signal transduction
POU1F1	5449	POU class 1 homeobox 1	Transcription regulation
PPARA	5465	peroxisome proliferator-activated receptor alpha	Metabolism
PRKCD	5580	protein kinase C, delta	Apoptosis
PTEN	5728	phosphatase and tensin homolog	Cell cycle
PTPN1	5770	protein tyrosine phosphatase, non-receptor type 1	Signal transduction
PTPN11	5781	protein tyrosine phosphatase, non-receptor type 11	Signal transduction
RET	5979	ret proto-oncogene	Cell cycle
RPA1	6117	replication protein A1	DNA damage repair
SHC1	6464	SHC transforming protein 1	Growth regulation
SST	6750	somatostatin	Growth regulation
STAT3	6774	signal transducer and activator of transcription 3	Transcription regulation
STAT5A	6776	signal transducer and activator of transcription 5A	Transcription regulation
STAT5B	6777	signal transducer and activator of transcription 5B	Transcription regulation
TCF3	6929	transcription factor 3	Transcription regulation
TP53	7157	tumor protein p53	Cancer
TXN	7295	thioredoxin	Cancer
VCP	7415	valosin containing protein	DNA damage repair
WRN	7486	Werner syndrome, RecQ helicase-like	DNA damage repair

Table S3 List of positively selected genes identified in long-lived species.

Branch	Gene	Model	LnL	2ΔlnL	p.adjust	Parameters	Positive Sites（pp > 0.8）
Heterocephalus glaber	*IL7R*	ModelA	-5355.063			ω_0 = 0.136 ω_1 = 1.0 ω_2 = 55.56	184 0.990**;
		ModelA Null	-5358.884	7.642	0.006	ω_0 = 0.136 ω_1 = 1.0 ω_2 = 1.0	
	DGAT1	ModelA	-7826.170			ω_0 = 0.037 ω_1 = 1.0 ω_2 = 206.344	271 0.995**;
		ModelA Null	-7831.196	10.051	0.002	ω_0 = 0.038 ω_1 = 1.0 ω_2 = 1.0	
	NGF	ModelA	-4700.352			ω_0 = 0.057 ω_1 = 1.0 ω_2 = 19.701	120 0.986*;
		ModelA Null	-4702.660	4.615	0.032	ω_0 = 0.057 ω_1 = 1.0 ω_2 = 1.0	
	SHC1	ModelA	-8468.794			ω_0 = 0.021 ω_1 = 1.0 ω_2 = 23.46	51 0.972*;
		ModelA Null	-8471.238	4.888	0.027	ω_0 = 0.021 ω_1 = 1.0 ω_2 = 1.0	
	STAT5A	ModelA	-11545.632			ω_0 = 0.022 ω_1 = 1.0 ω_2 = 435.158	519 0.901; 603 0.985*;
		ModelA Null	-11548.466	5.669	0.017	ω_0 = 0.022 ω_1 = 1.0 ω_2 = 1.0	
Balaena mysticetus	*GSK3B*	ModelA	-4458.212			ω_0 = 0.01 ω_1 = 1.0 ω_2 = 999.0	57 0.840; 118 0.841;
		ModelA Null	-4460.432	4.440	0.035	ω_0 = 0.01 ω_1 = 1.0 ω_2 = 1.0	
Homo sapiens	*EMD*	ModelA	-1585.090			ω_0 = 0.066 ω_1 = 1.0 ω_2 = 325.92	6 0.996**;
		ModelA Null	-1588.927	7.674	0.006	ω_0 = 0.065 ω_1 = 1.0 ω_2 = 1.0	
Pongo abelii	*PPARA*	ModelA	-9645.415			ω_0 = 0.023 ω_1 = 1.0 ω_2 = 8.497	220 0.978*; 222 0.992**; 223 0.838; 291 0.989*;
		ModelA Null	-9649.334	7.838	0.005	ω_0 = 0.023 ω_1 = 1.0 ω_2 = 1.0	
	EGR1	ModelA	-8655.636			ω_0 = 0.032 ω_1 = 1.0 ω_2 = 10.739	83 0.994**; 95 0.996**; 313 0.967*; 415 0.562; 417 0.987*;
		ModelA Null	-8660.138	9.005	0.003	ω_0 = 0.031 ω_1 = 1.0 ω_2 = 1.0	
	GSS	ModelA	-7345.481			ω_0 = 0.064 ω_1 = 1.0 ω_2 = 999.0	
		ModelA Null	-7347.529	4.097	0.043	ω_0 = 0.063 ω_1 = 1.0 ω_2 = 1.0	

	GHR	ModelA	-9180.019			$\omega_0 = 0.092$ $\omega_1 = 1.0$ $\omega_2 = 11.079$	59 0.867; 118 0.823; 124 0.830; 156 R 0.927; 160 0.826; 205 1.000**;
		ModelA Null	-9184.384	8.729	0.003	$\omega_0 = 0.092$ $\omega_1 = 1.0$ $\omega_2 = 1.0$	
	STAT5B	ModelA	-11534.536			$\omega_0 = 0.015$ $\omega_1 = 1.0$ $\omega_2 = 12.221$	625 0.962*; 627 0.988*;
		ModelA Null	-11538.173	7.274	0.007	$\omega_0 = 0.015$ $\omega_1 = 1.0$ $\omega_2 = 1.0$	
Microcebus murinus	*HELLS*	ModelA	-12118.730			$\omega_0 = 0.046$ $\omega_1 = 1.0$ $\omega_2 = 73.435$	267 0.956*; 271 0.916;
		ModelA Null	-12123.525	9.590	0.002	$\omega_0 = 0.045$ $\omega_1 = 1.0$ $\omega_2 = 1.0$	
	ATF2	ModelA	-6527.743			$\omega_0 = 0.025$ $\omega_1 = 1.0$ $\omega_2 = 44.668$	295 0.839;
		ModelA Null	-6530.159	4.832	0.028	$\omega_0 = 0.025$ $\omega_1 = 1.0$ $\omega_2 = 1.0$	
	PLAU	ModelA	-8085.969			$\omega_0 = 0.055$ $\omega_1 = 1.0$ $\omega_2 = 10.305$	12 0.987*; 30 0.992**;
		ModelA Null	-8087.895	3.852	0.050	$\omega_0 = 0.054$ $\omega_1 = 1.0$ $\omega_2 = 1.0$	
	NCOR1	ModelA	-33035.937			$\omega_0 = 0.044$ $\omega_1 = 1.0$ $\omega_2 = 909.062$	1377 0.991**; 1533 0.995**; 1536 M 0.992**; 1547 0.993**; 1548 0.992**;
		ModelA Null	-33055.111	38.347	0.000	$\omega_0 = 0.043$ $\omega_1 = 1.0$ $\omega_2 = 1.0$	
Callithrix jacchus	*ATM*	ModelA	-47199.353			$\omega_0 = 0.091$ $\omega_1 = 1.0$ $\omega_2 = 28.599$	164 0.962*;
		ModelA Null	-47203.736	8.766	0.003	$\omega_0 = 0.091$ $\omega_1 = 1.0$ $\omega_2 = 1.0$	
	ERCC6	ModelA	-18105.947			$\omega_0 = 0.046$ $\omega_1 = 1.0$ $\omega_2 = 9.473$	220 0.982*; 787 0.951*;
		ModelA Null	-18107.924	3.953	0.047	$\omega_0 = 0.046$ $\omega_1 = 1.0$ $\omega_2 = 1.0$	
	CREBBP	ModelA	-32203.266			$\omega_0 = 0.029$ $\omega_1 = 1.0$ $\omega_2 = 999.0$	1220 0.992*; 1221 0.972*; 1222 0.953*;
		ModelA Null	-32213.183	19.834	0.000	$\omega_0 = 0.029$ $\omega_1 = 1.0$ $\omega_2 = 1.0$	
Macaca nemestrina	*ERBB2*	ModelA	-22231.960			$\omega_0 = 0.04$ $\omega_1 = 1.0$ $\omega_2 = 147.608$	536 0.984*; 538 0.983*;
		ModelA Null	-22242.961	22.002	0.000	$\omega_0 = 0.04$ $\omega_1 = 1.0$ $\omega_2 = 1.0$	
Choloepus hoffmanni	*VCP*	ModelA	-11067.049			$\omega_0 = 0.001$ $\omega_1 = 1.0$ $\omega_2 = 8.211$	630 0.975*;

		ModelA Null	-11069.586	5.074	0.024	$\omega_0 = 0.001$ $\omega_1 = 1.0$ $\omega_2 = 1.0$	
	PDGFRB	ModelA	-19634.792			$\omega_0 = 0.041$ $\omega_1 = 1.0$ $\omega_2 = 3.404$	157 0.993**; 200 0.993**; 202 0.995**; 203 0.992**; 223 0.996**; 227 0.889; 230 0.977*; 235 0.991**; 320 0.985*; 348 0.838; 411 0.962*;
		ModelA Null	-19638.735	7.886	0.005	$\omega_0 = 0.041$ $\omega_1 = 1.0$ $\omega_2 = 1.0$	
	FOXO4	ModelA	-6679.140			$\omega_0 = 0.073$ $\omega_1 = 1.0$ $\omega_2 = 37.485$	37 0.848; 164 0.849; 169 0.835; 227 0.811; 330 0.826;
		ModelA Null	-6681.398	4.517	0.034	$\omega_0 = 0.072$ $\omega_1 = 1.0$ $\omega_2 = 1.0$	
	IGF1	ModelA	-1755.382			$\omega_0 = 0.032$ $\omega_1 = 1.0$ $\omega_2 = 25.79$	81 0.995**;
		ModelA Null	-1757.452	4.140	0.042	$\omega_0 = 0.031$ $\omega_1 = 1.0$ $\omega_2 = 1.0$	
	PTPN1	ModelA	-4097.124			$\omega_0 = 0.022$ $\omega_1 = 1.0$ $\omega_2 = 11.213$	148 0.999**; 150 0.989*;
		ModelA Null	-4100.872	7.496	0.006	$\omega_0 = 0.022$ $\omega_1 = 1.0$ $\omega_2 = 1.0$	
	APOE	ModelA	-4064.174			$\omega_0 = 0.097$ $\omega_1 = 1.0$ $\omega_2 = 11.505$	22 0.934; 100 0.974*; 145 0.969*;
		ModelA Null	-4067.841	7.335	0.007	$\omega_0 = 0.097$ $\omega_1 = 1.0$ $\omega_2 = 1.0$	
Myotis lucifugus	*CTGF*	ModelA	-4684.116			$\omega_0 = 0.028$ $\omega_1 = 1.0$ $\omega_2 = 52.795$	253 0.987*;
		ModelA Null	-4686.771	5.310	0.021	$\omega_0 = 0.028$ $\omega_1 = 1.0$ $\omega_2 = 1.0$	
	BCL2	ModelA	-2485.926			$\omega_0 = 0.03$ $\omega_1 = 1.0$ $\omega_2 = 999.0$	60 0.990*;
		ModelA Null	-2489.412	6.971	0.008	$\omega_0 = 0.028$ $\omega_1 = 1.0$ $\omega_2 = 1.0$	
	GHRH	ModelA	-1064.223			$\omega_0 = 0.112$ $\omega_1 = 1.0$ $\omega_2 = 25.548$	30 0.960*; 37 0.865;
		ModelA Null	-1066.620	4.793	0.029	$\omega_0 = 0.111$ $\omega_1 = 1.0$ $\omega_2 = 1.0$	
	PDGFRB	ModelA	-19994.262			$\omega_0 = 0.041$ $\omega_1 = 1.0$ $\omega_2 = 890.292$	534 0.976*; 536 0.830; 537 0.984*;
		ModelA Null	-20003.164	17.804	0.000	$\omega_0 = 0.042$ $\omega_1 = 1.0$ $\omega_2 = 1.0$	
	PLCG2	ModelA	-20036.080			$\omega_0 = 0.024$ $\omega_1 = 1.0$ $\omega_2 = 398.617$	665 0.962*;
		ModelA Null	-20040.208	8.256	0.004	$\omega_0 = 0.024$ $\omega_1 = 1.0$ $\omega_2 = 1.0$	

	DBN1	ModelA	-6652.028			$\omega_0 = 0.023$ $\omega_1 = 1.0$ $\omega_2 = 998.998$	244 0.991**;
		ModelA Null	-6655.057	6.058	0.014	$\omega_0 = 0.022$ $\omega_1 = 1.0$ $\omega_2 = 1.0$	
	ERCC3	ModelA	-12103.038			$\omega_0 = 0.011$ $\omega_1 = 1.0$ $\omega_2 = 6.5$	623 0.978*; 626 0.959*;
		ModelA Null	-12105.404	4.731	0.030	$\omega_0 = 0.011$ $\omega_1 = 1.0$ $\omega_2 = 1.0$	
	ABL1	ModelA	-15096.886			$\omega_0 = 0.02$ $\omega_1 = 1.0$ $\omega_2 = 769.282$	518 0.951*;
		ModelA Null	-15099.527	5.283	0.022	$\omega_0 = 0.02$ $\omega_1 = 1.0$ $\omega_2 = 1.0$	
	CTGF	ModelA	-4627.497			$\omega_0 = 0.029$ $\omega_1 = 1.0$ $\omega_2 = 23.054$	248 0.986*;
		ModelA Null	-4629.796	4.598	0.032	$\omega_0 = 0.029$ $\omega_1 = 1.0$ $\omega_2 = 1.0$	
	EGFR	ModelA	-20310.597			$\omega_0 = 0.039$ $\omega_1 = 1.0$ $\omega_2 = 8.506$	145 0.824; 274 0.973*; 309 0.956*; 371 0.971*;
Myotis brandtii		ModelA Null	-20313.278	5.363	0.021	$\omega_0 = 0.038$ $\omega_1 = 1.0$ $\omega_2 = 1.0$	
	DBN1	ModelA	-6674.313			$\omega_0 = 0.02$ $\omega_1 = 1.0$ $\omega_2 = 998.999$	247 0.991**; 251 0.569;
		ModelA Null	-6676.998	5.370	0.020	$\omega_0 = 0.02$ $\omega_1 = 1.0$ $\omega_2 = 1.0$	
	ABL1	ModelA	-15365.754			$\omega_0 = 0.02$ $\omega_1 = 1.0$ $\omega_2 = 999.0$	514 0.952*;
		ModelA Null	-15368.346	5.184	0.023	$\omega_0 = 0.02$ $\omega_1 = 1.0$ $\omega_2 = 1.0$	

Table S4 List of 16 unique positively selected genes identified in long-lived species none in the Control group.

Branch	Gene	Model	LnL	2ΔlnL	p.adjust	Parameters	Positive Sites（pp > 0.8）
Heterocephalus glaber	*SHC1*	ModelA	-8468.794			ω_0 = 0.021 ω_1 = 1.0 ω_2 = 23.46	51 0.972*;
		ModelA Null	-8471.238	4.888	0.027	ω_0 = 0.021 ω_1 = 1.0 ω_2 = 1.0	
Homo sapiens	*EMD*	ModelA	-1585.090			ω_0 = 0.066 ω_1 = 1.0 ω_2 = 325.92	6 0.996**;
		ModelA Null	-1588.927	7.674	0.006	ω_0 = 0.065 ω_1 = 1.0 ω_2 = 1.0	
Pongo abelii	*PPARA*	ModelA	-9645.415			ω_0 = 0.023 ω_1 = 1.0 ω_2 = 8.497	220 0.978*; 222 0.992**; 223 0.838; 291 0.989*;
		ModelA Null	-9649.334	7.838	0.005	ω_0 = 0.023 ω_1 = 1.0 ω_2 = 1.0	
	EGR1	ModelA	-8655.636			ω_0 = 0.032 ω_1 = 1.0 ω_2 = 10.739	83 0.994**; 95 0.996**; 313 0.967*; 415 0.562; 417 0.987*;
		ModelA Null	-8660.138	9.005	0.003	ω_0 = 0.031 ω_1 = 1.0 ω_2 = 1.0	
	STAT5B	ModelA	-11534.536			ω_0 = 0.015 ω_1 = 1.0 ω_2 = 12.221	625 0.962*; 627 0.988*;
		ModelA Null	-11538.173	7.274	0.007	ω_0 = 0.015 ω_1 = 1.0 ω_2 = 1.0	
Microcebus murinus	*HELLS*	ModelA	-12118.730			ω_0 = 0.046 ω_1 = 1.0 ω_2 = 73.435	267 0.956*; 271 0.916;
		ModelA Null	-12123.525	9.590	0.002	ω_0 = 0.045 ω_1 = 1.0 ω_2 = 1.0	
Callithrix jacchus	*NCOR1*	ModelA	-33035.937			ω_0 = 0.044 ω_1 = 1.0 ω_2 = 909.062	1377 0.991**; 1533 0.995**; 1536 M 0.992**; 1547 0.993**; 1548 0.992**;
		ModelA Null	-33055.111	38.347	0.000	ω_0 = 0.043 ω_1 = 1.0 ω_2 = 1.0	
Macaca nemestrina	*ERBB2*	ModelA	-22231.960			ω_0 = 0.04 ω_1 = 1.0 ω_2 = 147.608	536 0.984*; 538 0.983*;
		ModelA Null	-22242.961	22.002	0.000	ω_0 = 0.04 ω_1 = 1.0 ω_2 = 1.0	
Choloepus hoffmanni	*VCP*	ModelA	-11067.049			ω_0 = 0.001 ω_1 = 1.0 ω_2 = 8.211	630 0.975*;
		ModelA Null	-11069.586	5.074	0.024	ω_0 = 0.001 ω_1 = 1.0 ω_2 = 1.0	

	FOXO4	ModelA	-6679.140			$\omega_0 = 0.073$ $\omega_1 = 1.0$ $\omega_2 = 37.485$	37 0.848; 164 0.849; 169 0.835; 227 0.811; 330 0.826;
		ModelA Null	-6681.398	4.517	0.034	$\omega_0 = 0.072$ $\omega_1 = 1.0$ $\omega_2 = 1.0$	
	IGF1	ModelA	-1755.382			$\omega_0 = 0.032$ $\omega_1 = 1.0$ $\omega_2 = 25.79$	81 0.995**;
		ModelA Null	-1757.452	4.140	0.042	$\omega_0 = 0.031$ $\omega_1 = 1.0$ $\omega_2 = 1.0$	
Myotis lucifugus	*CTGF*	ModelA	-4684.116			$\omega_0 = 0.028$ $\omega_1 = 1.0$ $\omega_2 = 52.795$	253 0.987*;
		ModelA Null	-4686.771	5.310	0.021	$\omega_0 = 0.028$ $\omega_1 = 1.0$ $\omega_2 = 1.0$	
	BCL2	ModelA	-2485.926			$\omega_0 = 0.03$ $\omega_1 = 1.0$ $\omega_2 = 999.0$	60 0.990*;
		ModelA Null	-2489.412	6.971	0.008	$\omega_0 = 0.028$ $\omega_1 = 1.0$ $\omega_2 = 1.0$	
	GHRH	ModelA	-1064.223			$\omega_0 = 0.112$ $\omega_1 = 1.0$ $\omega_2 = 25.548$	30 0.960*; 37 0.865;
		ModelA Null	-1066.620	4.793	0.029	$\omega_0 = 0.111$ $\omega_1 = 1.0$ $\omega_2 = 1.0$	
	ERCC3	ModelA	-12103.038			$\omega_0 = 0.011$ $\omega_1 = 1.0$ $\omega_2 = 6.5$	623 0.978*; 626 0.959*;
		ModelA Null	-12105.404	4.731	0.030	$\omega_0 = 0.011$ $\omega_1 = 1.0$ $\omega_2 = 1.0$	
	DBN1	ModelA	-6652.028			$\omega_0 = 0.023$ $\omega_1 = 1.0$ $\omega_2 = 998.998$	244 0.991**;
		ModelA Null	-6655.057	6.058	0.014	$\omega_0 = 0.022$ $\omega_1 = 1.0$ $\omega_2 = 1.0$	
Myotis brandtii	*CTGF*	ModelA	-4627.497			$\omega_0 = 0.029$ $\omega_1 = 1.0$ $\omega_2 = 23.054$	248 0.986*;
		ModelA Null	-4629.796	4.598	0.032	$\omega_0 = 0.029$ $\omega_1 = 1.0$ $\omega_2 = 1.0$	
	DBN1	ModelA	-6674.313			$\omega_0 = 0.02$ $\omega_1 = 1.0$ $\omega_2 = 998.999$	247 0.991**; 251 0.569;
		ModelA Null	-6676.998	5.370	0.020	$\omega_0 = 0.02$ $\omega_1 = 1.0$ $\omega_2 = 1.0$	

Table S5 List of positively selected genes identified in the Control group (lifespan with non-increased).

Branch	Gene	ModelA LnL	ModelA Null LnL	2ΔLnL	P.adj	ω	Positive Sites (pp > 0.8)
Monodelphis domestica	*C1QA*	-5538.881	-5545.187	12.610	0.000	999.000	73 0.867;
	CDKN2B	-1863.771	-1865.890	4.237	0.040	999.000	
	E2F1	-2392.934	-2395.489	5.111	0.024	172.285	13 0.958*; 120 0.996**;
	EPOR	-6314.556	-6317.221	5.331	0.021	999.000	
	GRN	-10086.825	-10089.485	5.320	0.021	6.174	82 0.997**; 218 0.937; 237 0.921; 361 0.928;
	PDGFRB	-19240.541	-19242.569	4.055	0.044	999.000	
	TCF3	-5075.225	-5079.541	8.633	0.003	999.000	37 0.900;
	WRN	-20595.302	-20597.668	4.732	0.030	3.803	122 0.815; 140 0.916; 179 0.880; 221 0.944; 754 0.930; 830 0.800;
Erinaceus europaeus	*ATP5O*	-5154.135	-5158.448	8.626	0.003	998.999	108 0.955*;
	EGFR	-19923.857	-19927.105	6.498	0.011	222.335	108 0.879; 362 0.992**;
	ERCC2	-9250.400	-9252.840	4.881	0.027	76.206	115 0.971*;
	IL7R	-5444.146	-5448.084	7.878	0.005	998.996	130 0.959*;
	IRS1	-17165.290	-17168.343	6.106	0.013	71.541	813 0.980*;
	PLCG2	-19713.551	-19716.032	4.962	0.026	193.319	529 0.848;973 0.958*;
	PRKCD	-10447.433	-10449.841	4.814	0.028	289.954	126 0.956*;
	WRN	-20593.655	-20597.108	6.905	0.009	48.257	46 0.977*;
Sorex araneus	*ATM*	-46023.593	-46025.930	4.675	0.031	71.039	1292 0.918;
	CSNK1E	-3547.007	-3550.472	6.929	0.008	131.183	196 S 0.999**;
	DGAT1	-7318.911	-7321.407	4.992	0.025	10.190	144 0.974*; 155 0.979*;
	EGFR	-19918.687	-19921.351	5.328	0.021	6.760	51 0.815; 61 0.969*; 273 0.979*; 311 0.974*;

	EPS8	-14962.767	-14966.722	7.910	0.005	373.849	530 0.817;
	ERCC6	-17724.447	-17726.886	4.878	0.027	999.000	185 0.975*;
	GRN	-10094.133	-10096.535	4.804	0.028	998.931	280 0.956*;
	GSS	-7146.296	-7153.182	13.772	0.000	26.969	172 0.995**; 177 0.870; 200 0.960*; 249 0.923;
	H2AFX	-2278.693	-2281.319	5.253	0.022	999.000	
	HRAS	-3295.259	-3298.141	5.763	0.016	80.693	170 0.991**;
	IGF1R	-22181.252	-22185.272	8.041	0.005	70.778	65 0.875; 140 0.841; 176 0.860; 285 0.970*; 534 0.914; 570 0.892; 707 0.978*;
	IRS1	-17163.660	-17165.692	4.065	0.044	15.888	545 0.932; 566 0.943; 649 0.900;
	LMNA	-9797.589	-9803.020	10.863	0.001	514.980	456 0.942; 463 0.986*; 587 0.990*;
	WRN	-20583.204	-20587.344	8.280	0.004	8.207	78 0.993**; 392 0.982*; 412 0.985*; 452 0.986*; 787 0.988*; 821 0.982*;
Felis catus	*APOE*	-3957.453	-3960.139	5.373	0.020	998.996	104 0.930;
	PLCG2	-19706.626	-19710.700	8.149	0.004	67.517	259 0.957*; 261 0.930; 443 0.942;
	WRN	-20565.656	-20584.162	37.013	0.000	30.642	108 0.903; 127 0.997**; 128 0.937;130 0.997**; 149 1.000**;154 0.998**; 156 0.999**; 239 0.946;408 0.809; 735 0.943;
Canis lupus familiaris	*APP*	-11003.084	-11006.903	7.639	0.006	136.604	7 0.991**;
	GRN	-10090.512	-10094.067	7.112	0.008	14.168	243 0.992**; 317 0.988*;
	NGF	-4527.964	-4531.354	6.780	0.009	25.363	122 0.874; 134 0.848; 147 0.996**;
Equus caballus	*C1QA*	-5543.481	-5545.757	4.551	0.033	5.377	47 0.925; 74 0.976*; 101 0.897; 103 0.965*;
	H2AFX	-2277.210	-2279.188	3.955	0.047	57.333	7 0.975*; 100 0.873;
	IRS1	-17153.003	-17165.938	25.871	0.000	999.000	845 0.991**; 846 0.978*; 847 0.807;
	PDGFRB	-19242.686	-19253.151	20.929	0.000	999.000	370 0.964*; 395 0.983*;

Vicugna pacos	*ATM*	-46018.456	-46025.051	13.190	0.000	999.000	
	POU1F1	-4055.775	-4058.869	6.188	0.013	56.107	109 0.940; 110 0.995**;
	WRN	-20594.354	-20596.545	4.382	0.036	12.190	41 0.832;
Balaenoptera acutorostrata	*CREBBP*	-31777.346	-31780.419	6.147	0.013	999.000	
	TP53	-6740.036	-6742.380	4.687	0.030	803.289	16 0.934; 256 0.774;
Physeter catodon	*PEX5*	-10500.399	-10502.424	4.051	0.044	34.021	176 0.979*;
	RET	-18990.461	-18993.624	6.326	0.012	999.000	
	WRN	-20587.788	-20593.753	11.930	0.001	57.266	28 0.932;103 0.936; 104 0.954*; 123 0.931; 313 0.932; 361 0.849; 391 0.937; 727 0.937;
Lipotes vexillifer	*CTNNB1*	-11720.807	-11728.532	15.450	0.000	41.950	232 0.998**; 237 0.998**; 241 0.998**;
Neophocaena asiaeorientalis	*EGFR*	-19922.900	-19925.149	4.499	0.034	51.671	449 0.974*;
	HBP1	-7063.837	-7067.297	6.919	0.009	999.000	
	PLCG2	-19713.812	-19717.161	6.698	0.010	100.437	349 0.863;
Tursiops truncatus	*ATF2*	-6389.079	-6398.543	18.928	0.000	999.000	229 0.864; 230 0.861; 231 0.985*; 233 0.862;
	RPA1	-7529.648	-7533.595	7.895	0.005	47.310	18 0.843; 20 0.947; 103 0.949; 165 0.937; 351 0.850;
Bos taurus	*ATF2*	-6397.059	-6403.995	13.872	0.000	999.000	291 0.989*;
	PLCG2	-19707.070	-19711.233	8.326	0.004	215.766	671 0.999**;
	STAT5A	-11169.276	-11173.284	8.017	0.005	999.000	564 0.839; 567 0.979*;
	TP53	-6737.635	-6739.930	4.591	0.032	17.863	217 0.803; 234 0.994**;
Ovis aries	*BLM*	-16541.616	-16543.674	4.115	0.042	19.666	310 0.959*;
	C1QA	-5546.774	-5549.762	5.974	0.015	39.244	167 0.996**;
	EFEMP1	-5816.921	-5823.437	13.034	0.000	999.000	91 0.987*;
	ERCC1	-3386.015	-3390.291	8.551	0.003	999.000	32 0.995**;
	ERCC6	-17723.956	-17726.237	4.563	0.033	27.178	524 0.805; 729 0.981*;

	FGFR1	-11324.135	-11331.225	14.181	0.000	561.209	29 0.984*;
	LMNA	-9755.026	-9775.625	41.199	0.000	200.920	216 0.833; 258 0.989*; 261 0.881; 265 1.000**; 266 0.996**; 268 1.000**; 271 0.989*; 273 0.999**;
	STAT5A	-11160.425	-11165.223	9.596	0.002	31.393	287 0.997**; 530 0.997**;
Pteropus vampyrus	*ERCC5*	-10725.028	-10728.066	6.076	0.014	999.000	102 0.952*;
	GTF2H2	-6238.838	-6242.162	6.649	0.010	34.116	331 0.998**;
	PLAU	-8042.448	-8045.076	5.255	0.022	19.959	111 0.986*;
	TP53	-6738.410	-6740.684	4.549	0.033	9.279	3 0.967*; 236 0.980*;
Oryctolagus cuniculus	*APOE*	-3955.420	-3959.370	7.899	0.005	998.999	30 0.995**;
	APP	-11007.255	-11009.516	4.523	0.033	857.138	64 0.822;
	ERCC1	-3382.099	-3384.199	4.199	0.040	8.279	32 0.997**; 33 0.997**;
Ochotona princeps	*BRCA1*	-6668.587	-6670.550	3.927	0.048	19.169	205 0.932;
	FGFR1	-11291.278	-11299.194	15.833	0.000	22.174	106 0.949; 293 0.996**; 313 0.959*; 315 0.995**; 317 0.996**; 322 1.000**;
	PTPN11	-7799.861	-7802.652	5.582	0.018	8.277	36 0.976*; 37 0.956*;
	TCF3	-5077.244	-5079.570	4.651	0.031	42.495	22 0.930; 30 0.854; 135 0.975*; 151 0.980*;
Cavia porcellus	*ABL1*	-14934.278	-14936.725	4.893	0.027	14.298	594 0.974*;
	BRCA1	-6668.680	-6670.745	4.131	0.042	124.250	90 0.917;
	CLOCK	-10373.627	-10377.753	8.252	0.004	33.836	540 0.978*; 542 0.960*;
	COQ7	-4030.303	-4033.199	5.793	0.016	15.511	30 0.995**; 132 0.931;
	GSK3B	-4550.408	-4562.021	23.227	0.000	396.636	269 0.999**; 270 0.995**;
	IL7R	-5446.285	-5448.529	4.488	0.034	50.989	22 0.912; 145 0.883;
	PTEN	-3919.257	-3921.259	4.004	0.045	999.000	211 0.947;
Rattus norvegicus	*APTX*	-4872.003	-4874.539	5.072	0.024	142.605	63 0.949;

	TP53	-6739.875	-6742.120	4.491	0.034	29.162	65 0.984*;
Mus musculus	*CDK1*	-4086.492	-4088.416	3.847	0.050	20.118	25 0.987*;
	ERCC5	-10720.589	-10724.764	8.351	0.004	998.999	439 0.940; 440 0.972*;
	PLCG2	-19713.235	-19716.547	6.623	0.010	29.784	446 0.951*;
	PTPN1	-3967.679	-3970.183	5.007	0.025	16.519	54 0.992**;
Carlito syrichta	*APP*	-11004.452	-11006.442	3.979	0.046	17.595	29 0.971*;
	ATM	-46020.707	-46022.678	3.942	0.047	6.273	947 0.863;
	ATR	-37799.307	-37801.665	4.716	0.030	26.025	1415 0.852; 1445 0.878; 2092 0.963*;
	BRCA1	-6666.566	-6669.328	5.524	0.019	20.846	46 0.922; 156 0.891; 190 0.870;
	CDKN1A	-2402.539	-2405.375	5.672	0.017	998.997	
	ERCC6	-17722.824	-17725.639	5.629	0.018	214.303	337 0.982*;
	PLCG2	-19712.406	-19714.546	4.282	0.039	63.187	279 0.947; 404 0.960*;
Dasypus novemcinctus	*FGFR1*	-11325.901	-11331.003	10.204	0.001	720.678	25 0.982*;
	PDGFB	-2522.677	-2526.832	8.311	0.004	25.259	91 0.995**; 95 0.996**; 100 0.996**;
	PDGFRB	-19249.314	-19251.419	4.211	0.040	12.923	234 0.952*; 324 0.978*; 342 0.978*;
	RET	-18991.404	-18993.583	4.357	0.037	513.465	15 0.959*;
	TP53	-6739.030	-6742.070	6.079	0.014	9.568	39 0.884; 45 0.831; 158 0.870; 212 0.907;
	TXN	-1842.886	-1846.297	6.822	0.009	998.999	37 0.998**;
Procavia capensis	*CCNA2*	-5425.443	-5430.899	10.912	0.001	999.000	77 0.806; 309 0.994**;
	ERCC8	-3368.939	-3373.330	8.782	0.003	999.000	207 0.996**;
	GRN	-10091.036	-10094.985	7.899	0.005	30.580	238 0.993**;
	GSS	-7142.769	-7149.881	14.223	0.000	18.826	64 0.993**;180 0.999**;
	HRAS	-3292.198	-3295.910	7.423	0.006	516.135	98 0.993**;
	IL7R	-5446.572	-5448.580	4.016	0.045	247.285	16 0.933;
	NGF	-4530.766	-4534.491	7.452	0.006	56.211	20 0.969*;

Loxodonta africana	*H2AFX*	-2275.081	-2277.260	4.359	0.037	152.949	7 0.983*; 100 0.916;
	HDAC3	-5300.482	-5303.360	5.756	0.016	15.752	189 0.995**; 191 0.935;
	INSR	-23208.190	-23219.297	22.214	0.000	999.000	751 0.986*; 752 0.981*; 753 0.983*; 1038 0.906;
Echinops telfairi	*ATR*	-37801.729	-37803.898	4.337	0.037	461.674	1310 0.964*;
	BSCL2	-5499.130	-5502.035	5.810	0.016	324.696	256 0.971*;
	GHR	-9029.318	-9031.404	4.171	0.041	29.614	71 0.881;
	HESX1	-2747.147	-2750.473	6.651	0.010	72.536	35 0.991**;
	LMNA	-9809.656	-9802.213	14.887	0.000	1.949	
	PDGFRB	-19251.301	-19253.511	4.422	0.035	998.998	64 0.961*; 271 0.978*;

Table S6. Lambda (λ) parameter estimates for life-history traits in mammals

Life-History Trait	**λ**	***P* (λ)[a]**
MLS	0.97	<0.001
BM	0.99	<0.001
LQ	0.97	0.004

[a] Significance of difference of the **λ** model.

Table S7. Summary of genes with a root-to-tip d_N/d_S significantly correlated with maximum lifespan (MLS), body mass (BM), longevity quotient (LQ).

formula	model	outlier sample	R^2	lambda	coefficient	p value	p value.robust	R^2.robust	p value.max
BM ~ BMI1	pgls	"Balaena_mysticetus"	0.2845	0.94	4.0224	0.0006	0.0004	0.311	0.0157
BM ~ CTNNB1	pgls	"Myotis_brandtii"	0.2076	1	5.1071	0.0035	0.0035	0.2126	0.0216
BM ~ E2F1	pgls	"Orcinus_orca"	0.1146	0.961	3.2092	0.0246	0.0066	0.1792	0.0203
BM ~ ERBB2	pgls	"Physeter_catodon"	0.1539	1	6.6927	0.0104	0.0043	0.1985	0.034
BM ~ IGF1	pgls	"Balaena_mysticetus"	0.227	0.983	-3.1432	0.0034	0.0045	0.2204	0.016
BM ~ IGF1R	pgls	"Loxodonta_african"	0.3368	0.849	-4.8164	0.0001	0.0001	0.3558	0.0003
BM ~ PDGFB	pgls	"Myotis_brandtii"	0.1799	0.931	7.015	0.0065	0.0028	0.2226	0.0091
LQ ~ CDK1	pgls	"Myotis_brandtii"	0.337	0.439	1.7315	0.0045	0.002	0.2435	0.0075
LQ ~ ERCC3	ols	"Myotis_brandtii"	0.1541	0	1.8044	0.0103	0.0024	0.2236	0.0085
LQ ~ HRAS	pgls	"Homo_sapiens"	0.2071	0.735	0.6264	0.0035	0.0005	0.2959	0.0045
LQ ~ INSR	ols	"Homo_sapiens"	0.2197	0	3.574	0.0023	0.0003	0.3103	0.0035
MLS ~ ARNTL	pgls	"Sorex_araneus"	0.1233	0.886	0.9055	0.022	0.0044	0.2029	0.0202
MLS ~ ATM	pgls	"Balaena_mysticetus"	0.1834	0.894	3.7153	0.0053	0.0025	0.2216	0.0517
MLS ~ BMI1	pgls	"Rattus_norvegicus"	0.2084	0.855	0.7916	0.0034	0.0008	0.2756	0.0034
MLS ~ CDK1	ols	"Mus_musculus"	0.369	0	0.7481	0.0001	0.0001	0.4139	0.0003
MLS ~ CTNNB1	pgls	"Sorex_araneus"	0.143	1	1.0173	0.0144	0.0014	0.2537	0.0079
MLS ~ ERCC3	pgls	"Equus_caballus"	0.1007	0.753	0.5619	0.0333	0	0.4039	0.001
MLS ~ ERCC5	pgls	"Balaena_mysticetus"	0.1829	0.673	1.6322	0.0054	0.0058	0.1851	0.088
MLS ~ NRG1	pgls	"Balaena_mysticetus"	0.1874	0.997	0.6153	0.0049	0.0018	0.2356	0.0589
MLS ~ STAT5A	ols	"Homo_sapiens"	0.4206	0	1.4094	0	0	0.4723	0

REFERENCES

1. Austad, S. (2010). Methusaleh's Zoo: how nature provides us with clues for extending human health span. J. Comp. Pathol. ***142***, S10-S21.
2. De Magalhães, J.P., Costa, J., and Church, G.M. (2007). An analysis of the relationship between metabolism, developmental schedules, and longevity using phylogenetic independent contrasts. J. Gerontol. A Biol. Sci. Med. Sci. ***62***, 149-160.
3. Tacutu, R., Thornton, D., Johnson, E., et al. (2018). Human Aging Genomic Resources: new and updated databases. Nucleic Acids Res. ***46***, D1083-D1090.
4. Scornavacca, C., Belkhir, K., Lopez, J., et al. (2019). OrthoMaM v10: scaling-up orthologous coding sequence and exon alignments with more than one hundred mammalian genomes. Mol. Biol. Evol. ***36***, 861-862.
5. Keane, M., Semeiks, J., Webb, A.E., et al. (2015). Insights into the evolution of longevity from the bowhead whale genome. Cell Rep. ***10***, 112-122.
6. Castresana, J. (2000). Selection of conserved blocks from multiple alignments for their use in phylogenetic analysis. Mol. Biol. Evol. ***17***, 540-552.
7. Fletcher, W., and Yang, Z. (2010). The effect of insertions, deletions, and alignment errors on the branch-site test of positive selection. Mol. Biol. Evol. ***27***, 2257-2267.
8. Talavera, G., and Castresana, J. (2007). Improvement of phylogenies after removing divergent and ambiguously aligned blocks from protein sequence alignments. Syst. Biol. ***56***, 564-577.
9. Yang, Z. (2007). PAML 4: phylogenetic analysis by maximum likelihood. Mol. Biol. Evol. ***24***, 1586-1591.
10. Kumar, S., Stecher, G., Suleski, M., et al. (2017). TimeTree: a resource for timelines, timetrees, and divergence times. Mol. Biol. Evol. ***34***, 1812-1819.
11. Zhang, J., Nielsen, R., and Yang, Z. (2005). Evaluation of an improved branch-site likelihood method for detecting positive selection at the molecular level. Mol. Biol. Evol. ***22***, 2472-2479.
12. Yang, Z., Wong, W.S., and Nielsen, R. (2005). Bayes empirical Bayes inference of amino acid sites under positive selection. Mol. Biol. Evol. ***22***, 1107-1118.
13. Weadick, C.J., and Chang, B.S. (2011). An improved likelihood ratio test for detecting site-specific functional divergence among clades of protein-coding genes. Mol. Biol. Evol. ***29***, 1297-1300.
14. Anisimova, M., and Yang, Z. (2007). Multiple hypothesis testing to detect lineages under positive selection that affects only a few sites. Mol. Biol. Evol. ***24***, 1219-1228.
15. Zhang, J., and Kumar, S. (1997). Detection of convergent and parallel evolution at the amino acid sequence level. Mol. Biol. Evol. ***14***, 527-536.
16. Zou, Z., and Zhang, J. (2015). Are convergent and parallel amino acid substitutions in protein evolution more prevalent than neutral expectations? Mol. Biol. Evol. ***32***, 2085-2096.
17. Sun, Y.-B. (2018). FasParser2: a graphical platform for batch manipulation of tremendous amount of sequence data. Bioinformatics ***34***, 2493-2495.
18. Natarajan, C., Projecto-Garcia, J., Moriyama, H., et al. (2015). Convergent evolution of hemoglobin function in high-altitude Andean waterfowl involves limited parallelism at the molecular sequence level. PLoS Genet. ***11***, e1005681.
19. Muntané, G., Farré, X., Rodríguez, J.A., et al. (2018). Biological processes modulating longevity across primates: a phylogenetic genome-phenome analysis. Mol. Biol. Evol. ***35***, 1990-2004.
20. Revell, L.J. (2012). phytools: an R package for phylogenetic comparative biology (and other things). Methods Ecol. Evol. ***3***, 217-223.

21. Orme, D., Freckleton, R., Thomas, G., and Petzoldt, T. (2013). The caper package: comparative analysis of phylogenetics and evolution in R. R package version ***5***, 1-36.
22. Montgomery, S., and Mundy, N. (2013). Microcephaly genes and the evolution of sexual dimorphism in primate brain size. J. Evol. Biol. ***26***, 906-911.
23. Ma, S., Yim, S.H., Lee, S.-G., et al. (2015). Organization of the mammalian metabolome according to organ function, lineage specialization, and longevity. Cell Metab. ***22***, 332-343.
24. Yu, G., Wang, L.-G., Han, Y., and He, Q.-Y. (2012). clusterProfiler: an R package for comparing biological themes among gene clusters. OMICS ***16***, 284-287.
25. Thissen, D., Steinberg, L., and Kuang, D. (2002). Quick and easy implementation of the Benjamini-Hochberg procedure for controlling the false positive rate in multiple comparisons. J. Educ. Behav. Stat. ***27***, 77-83.
26. Szklarczyk, D., Gable, A.L., Lyon, D., et al. (2019). STRING v11: protein–protein association networks with increased coverage, supporting functional discovery in genome-wide experimental datasets. Nucleic Acids Res. ***47***, D607-D613.